RSC Pharmaceutics

ROYAL SOCIETY OF CHEMISTRY

PAPER

View Article Online
View Journal | View Issue

Cite this: *RSC Pharm.*, 2025, **2**, 1558

Novel zwitterionic densely charged neutral sulfobetaine polymeric micelles for oral delivery of therapeutic peptides: a proof-of-concept study

Muthanna Abdulkarim,*[a,b] Cátia Neto,[a] Flavia Laffleur,[c] Victor Ramos-Pérez,[d] Andreas Bernkop-Schnürch,[c] Salvador Gómez Borros[e] and Mark Gumbleton[a]

Densely charged but neutral sulfobetaine polymeric micelles (PMs) were designed with the aim of efficiently permeating the intestinal mucus and releasing the intact peptide cargo close to the intestinal epithelial surface. Using RAFT chemistry, butyl methacrylate and dimethyl aminoethyl methacrylate copolymers were synthesised and then reacted with propane sultone to form amphiphilic block copolymers comprising hydrophilic zwitterionic sulfobetaine and lipophilic butyl methacrylate (BMA). Small (diameter <50 nm), spherical BMA–sulfobetaine PMs with a near neutral surface charge potential and loaded with a model peptide cargo, the GLP1-agonist peptide exenatide, were then formed by nanoprecipitation. *In vitro* peptide release studies from the PMs showed that less than 0.9% of the peptide load was released within the first 2 h (*i.e.* there was no 'burst' effect), with the release unaffected by highly acidic conditions. Thereafter, a sustained release was evident with 43% of the peptide load released in 24 h. *In vitro* screening (cytotoxicity assay) showed that the PMs did not cause loss of epithelial cell viability. Multiple particle tracking showed that the PMs were very highly permeant through the intestinal mucus. An *in vivo* non-clinical rodent pharmacokinetic study demonstrated the oral delivery of the exenatide-loaded PMs to achieve an extent of peptide bioavailability of 13% relative to subcutaneous (s.c.) exenatide solution injection. A pharmacodynamic study showed the efficacy of the oral exenatide-loaded PMs with significant reductions in blood glucose following a glucose challenge test. In conclusion, a novel family of sulfobetaine PMs have been demonstrated as stable carriers, efficiently permeating the intestinal mucus and with the potential for exploitation in the oral delivery of therapeutic peptides.

Received 9th July 2024,
Accepted 25th August 2025

DOI: 10.1039/d4pm00202d

rsc.li/RSCPharma

1. Introduction

Efficient oral absorption of polypeptide-based therapeutics is challenged by not only by the lack of permeability of the intestinal epithelium to such agents but also the harsh environment of the gastro-intestinal lumen.[1,2] Compared to other mucosal barriers, the intestinal mucus is thicker with higher mechanical strength due to the condensed mucin fibre network[3] which has a mesh size ranging from 1000 nm down to less than 100 nm (ref. 4) within which other intestinal mucus constituents (lipids, proteins and DNA) either exist freely within the voids of the network or are adsorbed to mucin fibres.[5] To reach the gastrointestinal (GI) absorption surface itself, therapeutic peptides must not only show stability to pH and enzymatic challenges but also diffuse through the mucus barrier.[6]

Currently there are more than 60 therapeutic polypeptides in the global market and over 150 agents at different stages of development.[7,8] Most of these peptides have short half-lives resulting in more frequently repeated daily injection doses that may impair patient adherence.[9] A major growth area in pharmaceutical technology is the oral delivery of peptide hormones. The potential for the oral administration of glucagon-like peptide 1 (GLP-1) agonists exemplifies the possibilities and need.[10] These agents can provide effective control of blood glucose levels and promote central satiety, leading to weight loss benefit, an outcome impacting not only type 2 dia-

[a]*School of Pharmacy & Pharmaceutical Sciences, Cardiff University, Cardiff CF14 3NB, UK*
[b]*Department of Pharmaceutical Sciences, College of Pharmacy, Alfaisal University, P. O. Box 50927, Riyadh 11533, Saudi Arabia. E-mail: malbaldawi@alfaisal.edu; Tel: +966 11 215 (8978)*
[c]*Department of Pharmaceutical Technology, Institute of Pharmacy, University of Innsbruck, Innrain 80/82, 6020 Innsbruck, Innsbruck, Austria*
[d]*International Business and Productive Unit Woundynamics and Hospital Care, IHT Group, 08185 Lliçà De Vall, Catalunya, Spain*
[e]*Grup d'Enginyeria de Materials (GEMAT), Institut Quimic de Sarrià, Universitat Ramon Llull, Via Augusta 390, 08017 Barcelona, Spain*

betes mellitus but also a number of other chronic conditions.[11,12] Currently, only one of the six marketed GLP-1 agonist products is administered orally (semaglutide)[13,14] with a reported extent of bioavailability of 1%.[15]

Nanoparticles (NPs) may efficiently protect orally delivered peptides in the gastro-intestinal lumen[16] although the strategy does not necessarily prevent the NPs from entrapment in the intestinal mucus and failure to reach the absorption surface.[17] Our strategy to improve the mucus permeation of nanocarriers is to design 'slippery nanocarriers' possessing a highly hydrophilic surface that can reduce interactions with lipophilic components of the mucus and enabling a closer and more prolonged apposition of the nanocarrier with the intestinal absorption surface.[18] The principle of 'slippery surface nanocarriers' mimics the capsid virus with a very dense distribution of closely aligned negative and positive surface charges, presenting to the exterior a hydrophilic surface that bears an overall near neutral electrical character.[19]

Polybetaines are zwitterionic (co)polymers characterized by the presence of electrically opposite groups in the same monomer unit;[20] each betaine monomer unit possesses a terminal anionic group next to an amino cationic group, with betaine monomers termed sulfobetaine when the anionic species is a sulphate group.[21] Previous studies have shown that sulfobetaine film coatings can form an anti-adherent densely charged layer which can minimise electrostatic or lipophilic interactions.[22,23] Recent work using carboxybetaine nanotechnology, in which the carboxyl group serves as the terminal anion, showed highly improved oral delivery of insulin.[24,25] Hence, synthesising nanosized micelles from sulfobetaine polymers could provide an oral delivery system with exceptional mucus permeation properties. While these sulfobetaine polymers are well known to be anti-bioadherant, the literature has to date not revealed any studies using sulfobetaine nanotechnology for oral delivery of peptides. The hypothesis of this study was therefore that slippery-surface sulfobetaine PMs would have enhanced mucus permeation, allowing these carriers to achieve close proximity to the oral absorption barrier itself, and providing efficient controlled oral delivery of a peptide, *e.g.* the model GLP-1 agonist exenatide.

For the chemistry in this study, we used the reversible addition fragmentation chain transfer (RAFT) technique to create precise size-controlled sulfobetaine polymeric micelles (PMs) bearing a surface chemistry that minimises mucus interactions through mimicking highly mucus-diffusive viruses. We first synthesised low molecular weight butyl methacrylate (BMA) to serve as the lipophilic segment for the sulfobetaine PMs prior to copolymerising the BMA polymer with different ratios of dimethyl aminoethyl methacrylate (DMAEMA). The BMA : DMAEMA copolymers were then reacted with 1,3-propane sultone to form block copolymers of BMA : sulfobetaine, again making a variety of PMs with different ratios of BMA to sulfobetaine, with the zwitterionic block serving as the hydrophilic component of the PMs.

With the aim of creating a range (different ratios of BMA : sulfobetaine) of small-diameter PMs with neutral surface charge that were highly permeant through the mucus, these PMs were physicochemically characterised using a Malvern Zetasizer Nano ZS and by transmission electron microscopy (TEM). The peptide loading capacity (LD%) and peptide (exenatide) release from the PMs were examined using standard *in vitro* techniques. The cytotoxicity of the PMs was studied in epithelial cell-culture models, and the diffusive properties of the PMs in the mucus was assessed by a state-of-the-art multiple particle tracking (MPT) technique. The pharmacokinetic (PK) and pharmacodynamic (PD) *in vivo* effectiveness of the PMs was assessed in a rodent model and with respect to the oral delivery of a medium length GLP-1 agonist peptide, exenatide; the PD impact of peptide delivery explored the responsiveness of the animals to a glucose-tolerance test after having been first exposed to the GLP-1 agonist exenatide delivered *via* oral and subcutaneous (s.c.) routes of administration.

2. Materials and methods

2.1. Materials

The following materials were obtained from Fisher Scientific: BMA, DMAEMA, 1,3-propane sultone, 2-cyano-2-propyl dodecyl trithiocarbonate, 2,2′-azobis(2-methylpropionitrile) (AIBN) and tetrahalose were purchased from Sigma-Aldrich. Methanol, dioxane, dimethyl sulfoxide (DMSO), hexane, tetrahydrofuran (THF), and Dulbecco's modified Eagle's medium (DMEM). The fluorescent dye Lumogen Red-305 was a gift from Nanomi, the Netherlands. Other routine chemicals NaCl, KCl, Na_2HPO_4, KH_2PO_4, NaOH and HCl were also obtained from Fisher Scientific. A dialysis tubing (MW cut-off 20 kDa), the 3-[4,5-dimethylthiazol-2-yl]-2,5-diphenyl-tetrazolium bromide salt (MTT) kit for cell viability testing, and pepsin (porcine gastric mucosa-derived) were from Sigma-Aldrich. Fetal bovine serum (FBS) and penicillin–streptomycin solution were from Gibco. Glass bottom imaging dishes (35 mm diameter dish with a glass coverslip with 1.5 mm thickness and 10 mm diameter) were from MatTek Corporation (USA). Exenatide acetate was from Carbosynth Limited, UK. The exenatide ELISA kit (exendin-4 (*Heloderma suspectum*) – chemiluminescent EIA kit) was from Phoenix Pharmaceuticals Inc. (USA).

2.2. Synthesis of the zwitterionic BMA–sulfobetaine polymer

2.2.1. Synthesis of the lipophilic BMA block polymer. The BMA block polymer was synthesized by RAFT chemistry using AIBN as the initiator, 2-cyano-2-propyl dodecyl tri-thiocarbonate as the chain transfer agent (CTA) and dioxane as the reaction medium (Scheme 1). Prior to the synthesis, AIBN was purified by recrystallization in cold methanol and the BMA monomer was purified by passing the monomer solution through a bed of aluminum oxide to eliminate stabilizers. Using the standard RAFT equation (eqn (1)) for the target MW of the desired polymer,[26] pilot experiments optimised the ratio of BMA : CTA : AIBN to 25 : 1 : 0.1, respectively, in

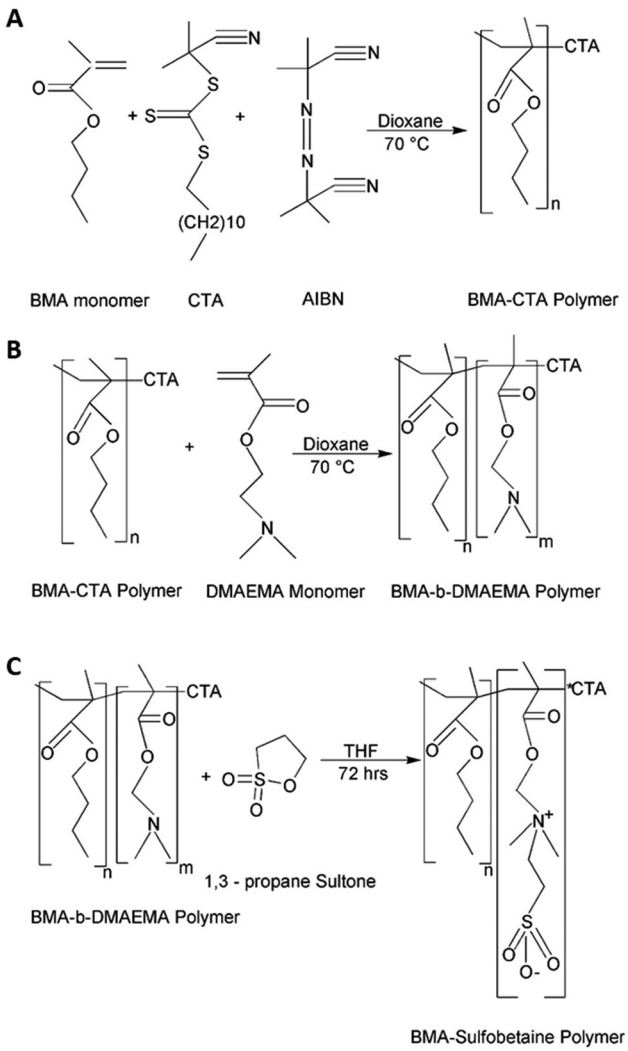

Scheme 1 Steps in the synthesis of BMA–sulfobetaine polymers, where the first step [A] includes the RAFT polymerisation of the BMA polymer using the CTA. The second step [B] includes the copolymerization of BMA–DMAEMA in which BMA–CTA serves as the macro-initiator to control the polymerisation of DMAEMA monomers. The third step [C] includes the synthesis of BMA–sulfobetaine, where the tertiary amino group of the DMAEMA unit was reacted with the γ carbon of 1,3 propane sultone.

order to synthesise BMA block polymers comprising 25 units per chain.

$$M_n = \left[\frac{\text{mole (monomer)}}{\text{mole (CTA)}}\right] \times \text{MW (monomer)} + \text{MW (CTA)} \quad (1)$$

In eqn (1), M_n = target MW of the polymer; [mole (monomer)/mole (CTA)] = molar ratio of the monomer to the CTA; MW (monomer) = MW of the monomer; and MW (CTA) = MW of the CTA.

For the synthesis using the optimized ratio, we first dissolved 3.52×10^{-3} moles of the BMA monomer, 1.40×10^{-4} moles of the CTA and 1.40×10^{-5} moles of AIBN in 2 ml of dioxane in a borosilicate glass tube. This medium was flushed with nitrogen gas for 30 min before the reaction was initiated by placing the tube in a silicon oil bath at 70 °C under continuous nitrogen flushing and 100 rpm stirring. The reaction was continued for 6 h (optimised in a pilot study) after which the reaction was stopped by exposure to air.

The BMA polymer produced was then purified by precipitation in excess cold methanol and centrifugation at 2600*g* for 20 min. The precipitate was washed twice with cold methanol and the supernatant was removed. The final precipitated polymer was dried under vacuum at room temperature ahead of the co-polymerisation steps.

2.2.2. Co-polymerisation of the BMA–DMAEMA di-block copolymer. The above dried BMA polymer was co-polymerised with DMAEMA monomers using RAFT chemistry to produce a size-controlled BMA–DMAEMA di-block copolymer. Here the BMA block polymer, holding the CTA, served as a macro-CTA[27] controlling the RAFT polymerisation of DMAEMA (Scheme 1). Using the ratios of reactants as defined by eqn (1), the BMA polymer was co-polymerized with DMAEMA to achieve the following five BMA–DMAEMA lipophilic di-block copolymer products differing in molar ratios (P is the polymer designation number): **P1**, 70 : 30; **P2**, 60 : 40; **P3**, 50 : 50; **P4**, 40 : 60; and **P5**, 30 : 70. The copolymerisation was carried out for 24 h under the same conditions of BMA polymerisation. The formed BMA–DMAEMA lipophilic di-block copolymers were precipitated in cold hexane (2600*g*) and the precipitates were washed twice in cold hexane prior to drying under vacuum pressure at room temperature.

2.2.3. Synthesis of the BMA–sulfobetaine di-block copolymer. In this step, each of the BMA–DMAEMA di-block copolymers (P1 to P5, above) was reacted with 1,3-propane sultone at a molar ratio of 1 : 2, respectively (Scheme 1). The reactions were conducted in THF for three days under mild stirring and under nitrogen as described for other sulfonation reactions.[28] The resultant BMA–sulfobetaine di-block copolymer was precipitated in excess acetone, centrifuged (2600*g*), and then washed twice with acetone before being left to dry under vacuum at room temperature. Each of the resulting BMA–sulfobetaine di-block copolymers was re-designated corresponding to the respective designations used above. Hence, the BMA : sulfobetaine di-block copolymers (with different molar ratios of BMA–DMAEMA) were designated respectively as **P1S** (70 : 30), **P2S** (60 : 40), **P3S** (50 : 50), **P4S** (40 : 60) and **P5S** (30 : 70).

2.2.4. Structural analysis of the synthesized polymer: NMR, IR and gel permeation chromatography (GPC). NMR spectra were recorded at 400 MHz (Varian NMR Instruments, Claredon Hills, IL) auto-calibrated to the deuterated solvent reference peak. The NMR spectrum was used to determine the degree of polymerization and purity of the synthesised polymers; $CDCl_3$ was the solvent in all NMR studies.

IR structural spectra were recorded using a Nicolet Magna 560 (Thermo Fisher Scientific, Waltham, MA) with a KBr beam splitter in an evaporated film.

GPC was performed to determine the polymer MW and polydispersity index (PDI). The analysis was performed using

an HPLC system (Elite LaChrom system, VWR-Hitachi) equipped with a GPC Shodex KF-603 column (6.0 mm ID, 150 mm) with THF as the mobile phase. The average MW (M_{w_a}) was calculated by comparing the retention time of each assessed polymer with the retention times of polystyrene standards. The polymer PDI was calculated using eqn (2):

$$\mathrm{PD} = \frac{M_{w_a}}{M_{n_a}} \quad (2)$$

where M_{w_a} = weight average MW and M_{n_a} = number average MW.

2.3. Preparation and characterisation of the zwitterionic sulfobetaine PMs

Sulfobetaine PMs were prepared using a modified nano-precipitation method in which the BMA–sulfobetaine di-block copolymers were dissolved in a mixture of organic and aqueous co-solvents. Instead of dissolving co-polymers in one solvent, solubilisation media for each di-block copolymer consisted of solutions comprising different ratios of 2 M NaCl to methanol.[29] The ratios of 2 M NaCl to methanol were based on the ratios of BMA to sulfobetaine in each copolymer. The ratios of 2 M NaCl : methanol were 50 : 50 for the P2S formulation, 55 : 45 for P3S, 65 : 35 for P4S and 75 : 25 for P5S. To form sulfobetaine PMs, 5 mg of each di-block co-polymer was dissolved in 500 μl of its specified 2 M NaCl : methanol solubilisation medium and then added dropwise at a rate of 20 μl min^{-1} into 5 ml of a stirred external aqueous phase (PBS pH 6.8) using a programmable syringe pump (Razel, USA). Upon completion, the formed PM suspension was stirred for a further 45 min to ensure the evaporation of methanol prior to PM physiochemical characterisation. Thereafter, sulfobetaine PMs were freeze-dried as follows: PM suspensions were dialysed (molecular weight cut-off, MWCO: 20 000) against 500 ml of PBS at pH 6.8 for 24 h followed by collection of the PM suspension in the dialysis tube. A cryo-protectant (tetrahalose) was added at a weight ratio of 5 : 1 to the total PM weight. The samples were freeze dried for 24 h (ref. 30) and then particle sizes and zeta potentials were measured. For any further studies, freeze dried samples were stored at 4 °C for further studies.

To track the particles using the MPT technique, the dye Lumogen Red was loaded into the PMs during their formation. Here, 5 μg of the dye was mixed with each copolymer prior to the nano-precipitation process.

Sulfobetaine PM characterisation involved the assessment of zeta potential and particle size using a Malvern Zetasizer Nano ZS, standardised using calibration standards. Particle size and zeta potential were measured using both freshly prepared sulfobetaine PMs and resuspended lyophilised PMs at time intervals following formation or resuspension of 0.5 h, 1 h, 2 h, 3 h, 4 h and 6 h at both 25 °C and 37 °C. Particle size and zeta potential were also measured before and after loading with Lumogen Red dye to assess the effect of freeze drying and loading of dye on the physicochemical properties of the particles.

While sulfobetaine PMs can be delivered within enteric-coated capsules to ensure greater protection of the peptide cargo against acid and pepsin, we undertook particle characterisation in acid and pepsin environments. Particle size was measured as above using resuspended lyophilised P5S PMs at 37 °C over a time of 2 h following resuspension. Sulfobetaine P5S PMs were suspended under four conditions: PBS buffer pH 7.2; PBS buffer pH 1.2; PBS buffer pH 7.2 + pepsin; and PBS buffer pH 1.2 + pepsin. The pepsin concentration employed was as previously described[31] for such experiments at a concentration of >800 I.U. per ml.

2.3.1. Micellar characterization by cryogenic transmission electron microscopy (cryo-TEM). The freezing of samples was conducted using an EM-CPC vitrification system (Leica Microsystems, Germany). A 4 μl sample aliquot was deposited onto a copper grid covered with a perforated polymer film. Any excess sample was removed with filter paper and then the grid was immersed in liquid ethane at 94 K. The vitreous sample was imaged using a JEOL JEM-2011 microscope (JEOL Ltd, Tokyo, Japan) operating at 120 kV. To avoid ice crystal formation during processing and imaging, the samples were maintained at a lower temperature (77 K).

2.4. Diffusion kinetics of sulfobetaine PMs within the intestinal mucus

PM diffusion through the intestinal mucus was assessed using a multiple particle tracking (MPT) technique using previously described mathematical and methodological approaches by our group.[32–35] Briefly, fresh samples (0.5 g) of porcine intestinal mucus were incubated in glass bottom MatTek imaging dishes at 37 °C. The fluorescently labelled PMs (*i.e.* those loaded with Lumogen Red) were inoculated into 0.5 g of mucus sample each in a reproducible manner that avoided particle aggregation at the point of inoculation. Particle tracking videos were captured using a high-speed camera (Allied Vision Technologies, UK) attached to a Leica DM IRB wide-field epifluorescence microscope (×63 magnification oil immersion lens). For each distinct PM formulation, a minimum of 360 individual micelle trajectories were tracked. These trajectories afforded calculation for each PM formulation: (i) a mean squared displacement (MSD) parameter; (ii) an ensemble mean squared displacement ⟨MSD⟩ parameter; (iii) an ensemble diffusion coefficient $\langle D_{eff} \rangle$ within the mucus; (iv) the proportion of the diffusive PMs within the mucus; and (v) the percentile heterogeneity of PM ensemble diffusion coefficients within the mucus. For the latter parameter, the individual micelle diffusions were ranked to allow comparison of, for example, the slowest (10^{th} percentile) to the fastest (90^{th} percentile) PMs; describing respectively the average effective diffusion for the slowest 10% of diffusion values, with the 90^{th} percentile is the average effective diffusion below which 90% of the D_{eff} values within the micelle population accrue. The PM diffusion coefficients in water (D°) were calculated using the Stokes–Einstein equation at a temperature of

37 °C. The diffusions of all PMs were also expressed by the % ratio $\langle D_{eff}\rangle/D°$.

2.5. Cytotoxicity of sulfobetaine PMs

The cytotoxicity of sulfobetaine PMs was tested using the MTT viability assay in the wild-type Madin–Darby Canine Kidney (MDCK-II) cells and in the Caco-2 epithelial line (European Collection of Authenticated Cell Cultures (ECACC)). The experiment was carried out following the protocol of the MTT kit supplier (Sigma-Aldrich). This assay is based on the ability of metabolically active cells to enzymatically reduce MTT salt to an insoluble coloured formazan crystal which is solubilised by addition of solubilisation buffer. The spectrophotometric quantification of the solubilised formazan is directly related to the quantity of the metabolically active cells. MDCK-II (passage 7) and Caco-2 (passage 20) cells were cultured under standard conditions (humidified atmosphere at 37 °C with 5% CO_2) using DMEM supplemented with 10% FBS and 1% penicillin–streptomycin.

For the MTT assay, MDCK and Caco-2 cells were seeded in 96-well plates (5×10^4 cells per well; 100 μl culture medium) and cultured for 24 h to reach confluence. Freeze-dried sulfobetaine PMs were then re-suspended in culture medium over a concentration range of 10^5 (polymer concentration of 10 ng ml^{-1} to 1 mg ml^{-1}). Two control arms were employed: (i) negative control – no treatment, *i.e.* lacking PMs, and (ii) positive control – no PMs but includes 1% Triton for complete cell lysis. Upon introduction of treatment (or controls), cells were incubated for 24 h after which 10 μl of the MTT reagent was added into each well, followed by further incubation for 4 h. Solubilisation buffer (100 μl) was then added into each well, followed by further incubation for 24 h to enable the solubilisation of any formazan crystals to fully proceed. The absorbance of the wells (corresponding to formazan turnover) was measured at a wavelength between 550 nm and 600 nm and a reference wavelength of 650 nm using an ELISA reader (LT-5000 MS, Taiwan).

2.6. Sulfobetaine PMs: ion-pairing, exenatide encapsulation and *in vitro* release kinetics of exenatide

The ion-pairing technique was utilised to adjust the physicochemical properties of the hydrophilic peptide exenatide for loading into the lipophilic core of the sulfobetaine PMs.[36] Ion pairing was carried out as follows: exenatide and sodium dodecyl sulphate (SDS) were solubilised separately in dilute glacial acetic acid solutions of the same pH values and then the SDS solution was added into the exenatide solution dropwise, followed by mixing for a further 2 h. Exenatide was mixed with SDS in two different pH solutions of dilute glacial acetic acid (pH 3.0 and pH 4.0) and at molar ratios of 3 : 1, 4 : 1 and 5 : 1 (Table 4). The formation of exenatide–dodecylsulphate was visually confirmed by the formation of a precipitate which was washed and centrifuged at 5000*g* twice, and then the powder was freeze dried for the next step.

To encapsulate exenatide–dodecylsulphate into the lipophilic core of the sulfobetaine PMs, 1 mg of each BMA–sulfobetaine polymer formula was dissolved in a 2 M NaCl : methanol solvent mixture, with the ratio of the solvents varying according to the ratios of BMA to sulfobetaine. For each 1 mg of PMs, 150 μg of exenatide–dodecylsulphate was dissolved in 75 μl of methanol. The solubilised polymer and exenatide–dodecylsulphate solutions were then added dropwise into an aqueous phase (PBS pH 6.8) to allow self-assembly of the PMs with the incorporation of exenatide into the PM core. The PM suspensions were then dialysed (dialysis tubing, MWCO: 20 000) against PBS pH 6.8 for 6 h and the exenatide entrapment efficiency (EE%) (eqn (3)) and % loading capacity (LD%) (eqn (4)) were calculated for the four different sulfobetaine PMs species, ranging from those with a large hydrophilic sulfobetaine segment (*i.e.* P5S) to a relatively small hydrophilic segment (*i.e.* P2S).

The exenatide concentration was measured as described by our group previously using the chemiluminescent ELISA technique (Phoenix Pharmaceuticals Inc., linear range of 1 picogram (pg)–10 ng mL^{-1}) using 50 μl of samples.[37]

$$\mathrm{EE}\,(\%) = \frac{\text{Amount of exenatide loaded into PM}}{\text{Total amount of exenatide}} \times 100 \quad (3)$$

$$\mathrm{LD}\,(\%) = \frac{\text{Amount of exenatide loaded into PM}}{\text{Total amount of exenatide available for loading}} \times 100 \quad (4)$$

All *in vitro* release studies were conducted using the dialysis tube method, which involved a 1 ml dialysis tube (MWCO: 20 kDa) against 200 ml of external media of PBS buffer pH 6.8 at 37 °C. Studies on the *in vitro* release of exenatide from all PM formulations (P2S, P3S, P4S and P5S) and the transfer of free exenatide acetate across the dialysis tubing were carried out initially for 8 h in PBS pH 6.8 (at or close to intestinal pH). All experiments involved 150 μg of exenatide as the initial drug mass (either free in solution as exenatide or loaded within PMs) and placed in each dialysis tube. For the PMs, this was 150 μg of exenatide loaded into 1 mg of PM mass making an overall 1.15 mg mass containing the polymer and 150 μg of peptide. Following the initial release studies, the PM formulation which showed the most optimum *in vitro* release profile (P5S) was subjected to more extended-release studies. They were conducted over 24 h in which the first 2 h studies were carried out in PBS buffer pH 1.2 and then the PM formulation was transferred to PBS buffer pH 6.8 for the following period between 2 and 24 h.

2.7. *In vivo* PK and PD studies in a rodent model

The *in vivo* efficacy of orally administered sulfobetaine–exenatide PMs was assessed in PK and PD studies using healthy male Sprague-Dawley rats following similar experimental procedures mentioned in our previous work.[37] All animal procedures were performed in accordance with the Guidelines for Care and Use of Laboratory Animals of the University of Innsbruck and approved by the Animal Ethics Committee of

Austria (Vienna) (BMWFW-66.008/0027-WF/V/3b/2016). Male Sprague-Dawley rats (mean BW 250–300 g) were obtained from Janvier Labs (Saint Berthevin, France). The animals were fasted 12 h prior to the experimental procedures and had free access to water throughout.

PK studies involved the measurement of exenatide plasma levels up to 10 h after exenatide administration. Ethical issues constrained the volume of blood that could be sampled across the full temporal profile of the PD and PK readouts; hence the PK study was undertaken in a different group of animals to those used for the PD studies. The PD studies included measuring blood glucose levels in response to administration of intraperitoneal (i.p.) injection of 2 g kg^{-1} glucose using 50% dextrose solution in sterile water (glucose challenge test – GCT).

Before conducting the full scale PK and PD studies, pilot investigations were conducted to determine: (i) the lower limit of quantification (LLQ) for PD measurements (glucose *via* Glucometer AccuCheck® Active, F. Hoffmann-La Roche AG) and for PK measurements (exenatide blood levels measured using ELISA, Phoenix Pharmaceuticals Inc.); (ii) the timing of peak glucose levels following the GCT; and (iii) the timing of the administration for each treatment arm involving exenatide (PMs, subcutaneous (s.c.) injection, oral solution) relative to peak glucose levels.

PK studies involved three treatment arms without GCT administration (n = 3 animals for each arm): (i) s.c. exenatide solution, dose 20 μg as above; (ii) oral sulfobetaine–exenatide PMs in a suspension, dose of 150 μg of exenatide (=1.15 mg PM mass within which was loaded 150 μg of exenatide); and (iii) oral exenatide solution dose of 150 μg of exenatide. Following exenatide administration, 200 μl of blood samples were withdrawn from the tail vein and plasma was separated and stored at −80 °C until analysis (maximum time between collection and analysis did not exceed three months). Blood sample collections were timed at 0 min, 0.5 h, 1 h, 1.5 h, 2 h, 3.5 h, 6 h, and 10 h after exenatide administration. The s.c. and oral doses of exenatide in the PK study were based on the pilot experiments and the LLQ of exenatide and drew some reference to previous studies performed on the oral and s.c. delivery of exenatide.[38–40]

For concentration analysis, exenatide was extracted from the plasma samples following the protocol described by Phoenix Pharmaceuticals Inc. Briefly, plasma samples (50 μl) were mixed with an equal volume of an acidic buffer (supplied by Phoenix) and centrifuged for 20 min at 17 000g (4 °C). The supernatants were extracted as per the protocol through an acidified C18 column with the acidic buffer. The eluent was then freeze-dried prior to measurement using luminescent immunoassay (ELISA – Phoenix Pharmaceuticals Inc.) which displayed a linear range of 1–10 000 pg ml^{-1}. Exenatide plasma concentration–time curves were plotted and the data were analysed through non-compartmental approaches. The relative bioavailability of the oral dosed exenatide was determined using eqn (5) from the plasma levels between time 0 h and the last collection of 10 h only.

$$F_{\text{oral relative}} = \frac{\text{AUC}_{\text{oral}} \times \text{Dose}_{\text{s.c}}}{\text{AUC}_{\text{s.c.}} \times \text{Dose}_{\text{oral}}} \quad (5)$$

Note: AUC based only on timepoints 0 to 10 h.

The PD studies involved four treatment arms (n = 4 animals for each arm): (i) GCT i.p. alone (no treatment) comprising the i.p. administration of 2 g kg^{-1} glucose; (ii) s.c. injection exenatide (dose 20 μg of exenatide into the thigh in 60 μl of PBS solution) 10 min prior to i.p. GCT; (iii) oral sulfobetaine–exenatide PMs (suspension as 1 ml oral gavage with exenatide–dodecylsulphate equal to 150 μg of exenatide dose) administered 4 h prior to i.p. GCT; and (iv) oral exenatide solution (dose 150 μg of exenatide as 1 ml oral gavage) administered 4 h prior to i.p. GCT.

When i.p. GCT followed exenatide administration, the time period between exenatide and i.p. GCT adminstrations was optimised such that peak (near-peak) exenatide plasma levels corresponded to the point of i.p. GCT injection.

For glucose analysis, 40 μl of blood samples were withdrawn from the tail vein at the following times: 0, 0.5 h, 1 h, 1.5 h, 2 h, 3 h, 4 h and 5 h after the respective i.p. administration of glucose as part of the GCT.

2.8. Statistical analysis

Statistical significance was obtained using PRISM10 GraphPad software. Cytotoxicity and baseline blood glucose level (at time 0) studies were performed using one-way ANOVA followed by Dunnett's multiple comparison test. Blood glucose levels studied (at different time-points) were assessed by two-way ANOVA with Tukey's multiple comparison test. P values are reported as follows: non-significant (ns) > 0.05; * ≤ 0.05; ** ≤ 0.01 and *** ≤ 0.001.

3. Results and discussion

3.1. Synthesis of the zwitterionic BMA–sulfobetaine polymer

Amphiphilic block co-polymers were synthesised using RAFT chemistry to modify the MW and hence the size of the lipophilic core (BMA) and hydrophilic shell (DMAEMA–sulfobetaine) within the PMs, an approach similar to that described previously.[41,42]

3.1.1. Synthesis of the lipophilic BMA block polymer. A low MW lipophilic polymer, such as the BMA polymer, forms the lipophilic core in the PMs,[43] affording the potential to form overall small diameter PMs.[44] Small lipophilic segments reduce the potential of micelle interaction with mucus components within the intestinal lumen, which may otherwise trap PMs through steric effects[45] or through lipophilic interactions with the cysteine domains of the mucus.[46]

Based on pilot studies, a ratio of 25 : 1 (BMA monomer : CTA) was used in RAFT chemistry to form 25 BMA units in each polymer chain. The ^{1}H-NMR spectrum of the BMA polymerised for 6 h (Fig. S1A) demonstrates the formation of 24 BMA units

(3988 Da), which is in accordance with GPC measurement (Fig. S1B). MW assessment of BMA using ^{1}H-NMR was undertaken by counting the number of BMA units (peak signal A at 3.85–3.95 ppm in the ^{1}H-NMR spectrum) *versus* a single CTA (1 unit) with a peak signal at 3.15 ppm (Fig. S1A). The ^{1}H-NMR spectrum of BMA also showed overnight polymerisation, resulting in an overgrown BMA polymer (56 units) (data not shown), which supported the observation that 6 h of polymerisation was the typical polymerisation time to achieve the desired (*ca.* 25 BMA units) degree of polymerisation.

Previous studies have shown that the duration of the RAFT chemistry reaction is critical to controlling the degree of polymerisation of active monomers such as BMA;[47] BMA is an active monomer that is known to grow under uncontrolled polymerisation to tens of thousands of grams per mole with very high polydispersity.[48] Reducing the time and selecting the appropriate CTA for the RAFT chemistry is essential to obtain a size and composition-controlled BMA polymer.

The GPC profile of BMA polymerised for 6 h (Fig. S1B) showed a MW of 3988 and a PDI of 1.28, which authenticates the suitability of the CTA (2-cyano-2-propyl dodecyl trithiocarbonate) for the controlled polymerisation of BMA (PDI being acceptable within the limit of ≤1.3).[27,49] Again, this is consistent with previous studies where the CTA bearing a cyano group has been widely reported for controlled RAFT polymerisation of active monomers such as BMA.[50–52]

3.1.2. Copolymerisation of the BMA–DMAEMA di-block copolymer. A CTA was used in the copolymerisation reaction to synthesise the BMA : DMAEMA di-block copolymer. Table 1 shows the calculated moles of BMA-CTA to DMAEMA reacted with the AIBN initiator for each of the BMA–DMAEMA lipophilic di-block copolymer products, *i.e.* P1 to P5, which represent, respectively, the BMA : DMAEMA molar ratios 70 : 30, 60 : 40, 50 : 50, 40 : 60, and 30 : 70. Fig. S2(A–E) shows the respective ^{1}H-NMR spectra of P1 to P5 copolymers. The ^{1}H-NMR spectra were used to determine (detect) the ratios of BMA to DMAEMA block polymers by comparing the area under the curve of the distinctive signal peak from BMA to that of DMAEMA. In Fig. S2, signal A (3.85–3.95 ppm) represents the methyl group adjacent to the ester groups in BMA, which was compared to signal B (4.15–4.25 ppm) representing the methyl group next to the ester group for DMAEMA (structural description presented to the left in Fig. S2). Table 1 shows the MW of BMA–DMAEMA copolymers detected using the ^{1}H-NMR spectrum by summing the MWs of units in each copolymer.

Comparing (Table 1) the molar ratios of BMA to DMAEMA detected by ^{1}H-NMR to those calculated using the RAFT equation showed a very high agreement *i.e.* the number of DMAEMA monomers copolymerised to BMA was consistent with the calculated ratios. This indicates that the degree of polymerisation of the DMAEMA polymer was efficiently controlled by the trithiocarbonate CTA, as in ref. 53; trithiocarbonate as a macro-CTA is broadly described as a good source for di-block and tri-block controlled copolymerisations.[54,55]

3.1.3. Synthesis of the BMA–sulfobetaine di-block copolymer. In this step, the DMAEMA block of each BMA–DMAEMA di-block copolymer was betainised by reacting with propane sultone. As shown in Scheme 1, each DMAEMA tertiary amino group was attached to the γ-methyl group of propane sultone to form a zwitterionic, highly charged, amphiphilic BMA–sulfobetaine copolymer. In the resulting di-block copolymer, the BMA and the ester part of DMAEMA form the hydrophobic segment and the hydrophilic zwitterionic sulfobetaine serves as the hydrophilic segment. The newly formed BMA–sulfobetaine copolymers were designated as P1S, P2S, P3S, P4S and P5S corresponding to the BMA–DMAEMA lipophilic di-block copolymers P1, P2, P3, P4 and P5, respectively.

IR analysis was used to investigate the step-by-step structural transformation of the BMA polymer into the BMA–DMAEMA copolymer through the formation of BMA–sulfobetaine copolymers (P2S, P3S, P4S and P5S). Fig. 1 shows the IR spectra of the BMA block polymer (1A), the BMA–DMAEMA di-block copolymer (1B) and the BMA–sulfobetaine copolymer (1C), in which the functional groups within the respective structures are highlighted. The presence of methyl (2850–3000 cm^{-1}), ether (1210–1320 cm^{-1}), ester (1750–1820 cm^{-1}) and amino (1080 cm^{-1}) functional groups indicates the formation of BMA block and BMA–DMAEMA copolymers (Fig. 1A and B). Consequently, the formation of sulfonyl (1030–1060 cm^{-1}) and sulfanol (3200–3550 cm^{-1}) groups confirmed the formation of BMA–sulfobetaine (Fig. 1C).

Moreover, it was clear that the rate of betainisation is related to the ratios of the BMA lipophilic block to DMAEMA. By observing the reactions over 72 h, copolymers with low ratios of BMA (P4S, P5S) were formed at a faster rate (precipitation within the first 24 h) compared to P3S with a slower rate (precipitation observed only after 48 h) and P1S and P2S, which showed no precipitation after 72 h. The addition of acetone to the reaction media increased the betainisation yield

Table 1 Calculated *versus* detected molar ratios of BMA to DMAEMA in the BMA–DMAEMA di-block copolymer synthesis

Formula	Calculated molar ratio of BMA : DMAEMA (n : m)	Calculated ratio of DMAEMA to CTA using the RAFT equation	BMA : DMAEMA molar ratio detected by NMR (n : m)	Ratio of the units in BMA : DMAEMA detected by NMR	MW of the copolymer detected by ^{1}H-NMR (g mol^{-1})
P1	(70 : 30)	10.2	69 : 31	24 : 10	5370
P2	(60 : 40)	16	58 : 42	24 : 16	6265
P3	(50 : 50)	24	49 : 51	24 : 24	7517
P4	(40 : 60)	36	39 : 61	24 : 36	9396
P5	(30 : 70)	56	28 : 72	24 : 56	12 528

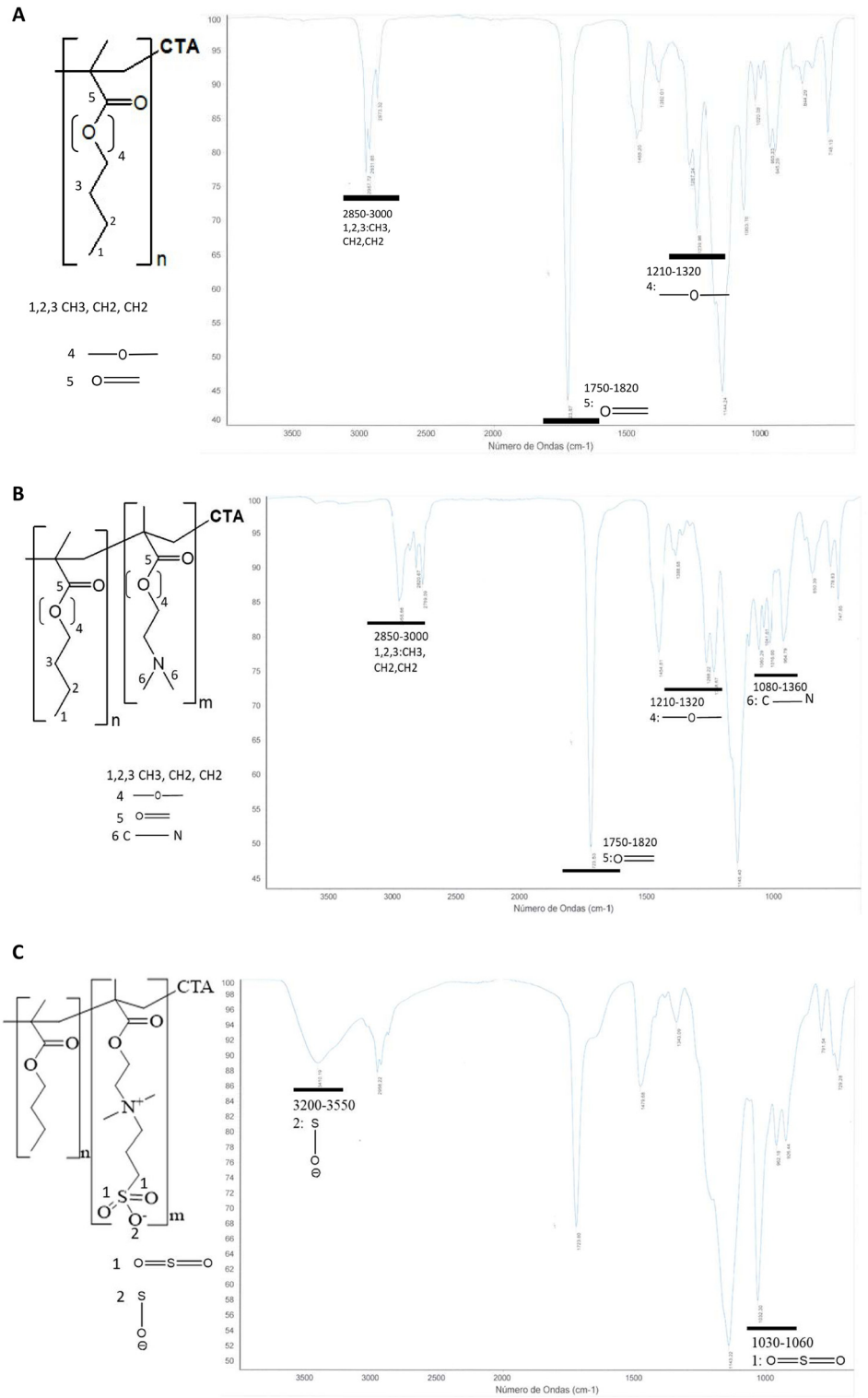

Fig. 1 Infra-red (IR) spectrum showing the structural characterisation of BMA–sulfobetaine with respect to step-by-step formation, where [A] shows the functional groups of BMA, [B] shows the functional groups of BMA–DMAEMA, while [C] shows the functional groups of BMA–sulfobetaine. Note: only the main functional groups were highlighted in each IR spectrum.

(precipitation) of all polymers, with the highest yield obtained for P5S followed by P4S, P3S and then P2S. P1S (70% BMA) showed negligible yields, meaning that the use of this polymer in the formulation of PMs is unreasonable (P1S was not used further for PM formation or study). The retarding effect of the lipophilic block polymer copolymerised with DMAEMA has

impacts on betainisation, and was described by Bütün *et al.* (1997)[56] showing that an increase in the ratio of the block polymer (2-diisopropylamino ethyl methacrylate) copolymerised to DMAEMA (from 20% to 40%) resulted in significant reduction in the betainisation of DMAEMA.[56] Bütün explained this effect by the steric action of the other block polymer, reducing the ability of the tertiary amine of DMAEMA to react with propane sultone.

3.2. Preparation and characterisation of the zwitterionic sulfobetaine PMs

Zwitterionic sulfobetaine PMs were prepared using the nano-precipitation method involving the solubilisation of the polymers in solvents, followed by the addition of the polymer solution to an external aqueous phase.[57] BMA–sulfobetaine is composed of lipophilic blocks of BMA and the ester part of DMAEMA, which is soluble in organic solvents. The very hydrophilic block, sulfobetaine, which is insoluble in any organic solvent, is soluble in the aqueous phase. Therefore BMA–sulfobetaine copolymers are insoluble in any mono-component solvent, and different mixtures of organic and aqueous solvents have to be examined to solubilise these zwitterionic polymers, as reported for other zwitterionic amphiphilic copolymers.[58] We found that using a mixture of 2 M NaCl with methanol was optimal to solubilise these copolymers (average solubility 10 mg ml^{-1}), with the ratio of the two solvents varying depending on the ratio of BMA to sulfobetaine. Optimising solubility is essential for producing more consistent and smaller-sized particles using the nano-precipitation method; an average solubility of 10 mg ml^{-1} was satisfactory in this study.[59,60] Using 2 M NaCl as the aqueous solvent resulted in higher solubilisation compared to water. This is explained by the anti-polyelectrolyte effect of NaCl,[20] describing the conformation of the zwitterionic polymer in an aqueous phase as a collapsed globular structure (due to dipolar interactions between the opposite charges – amino and sulphate groups). The addition of low MW electrolytes such as NaCl can screen these dipolar interactions, resulting in a polymer adopting an extended conformation, which enables an organic solvent such as methanol to access and solubilise the lipophilic block, which would be hidden in the collapsed globular structure.

Solubilised copolymers were later nano-precipitated in an external phase of PBS pH 6.8 to mimic the intestinal pH (Table 2). After the formation of PMs, particle sizes and zeta potentials were measured at temperatures of 25 °C and 37 °C. Stability in these parameters was studied over 6 h (0.5, 1, 2, 3, 4 and 6 h) to encompass the time of gastric to distal small intestinal transit of particles administered orally to the rat.[61,62] Similarly, the effect of freeze drying on the sulfobetaine PM was explored by measuring the particle size and zeta potential over 6 hours after resuspension from the lyophilised state. The impact of the inclusion of Lumogen red (fluorescent dye) loading on the particle size and zeta potential was also studied.

Table 2 shows that all sulfobetaine PMs displayed particle sizes below 50 nm with the smallest being 28 nm for the P2S formulation comprising 60% BMA. The associated polydispersity indices ranged between 0.42 and 0.48, indicating a relatively broad distribution. This is mainly due to the very rapid precipitation of the PMs by the nano-precipitation drop-wise approach, which leads to a greater level of heterogeneity with the formation of a very small percentage of polymeric aggregates,[63] which, in this study, were not subjected to further filtration removal. The zeta potentials of these PMs were, as predicted by the chemical strategy, close to neutrality with only slightly negative values of −0.57 to −2.26 mV. As mentioned, the small size of the BMA–sulfobetaine PMs is associated with a smaller MW of the lipophilic block.[64] For example, as others have found, if the lipophilic block is smaller than 9000 Da, micelle-like polymeric structures are formed with small particle sizes;[65,66] in our own work with BMA–sulfobetaine PMs the MW of the BMA lipophilic block polymer is only 3500 Da. Previous studies have reported the synthesis of self-assembled zwitterionic sulfobetaine particles with sizes less than 50 nm.[67,68] The near neutral charge of the BMA–sulfobetaine PMs indicates complete betainisation of the DMAEMA polymer, where each positively charged amino group is neutralised by a negatively charged sulfonate group on the same polymer chain.[69] The slight negativity of these PMs is the result of the 'chameleon effect',[70] where very small amounts of anions from the external media can be adsorbed onto the surface of the sulfobetaine polymer.[71]

Table 2 also shows that compared to the freshly assembled dye-free PMs, the Lumogen Red dye loading (at a low concentration of 0.1% w/w) lacked any impact on the physicochemical properties of the PMs, consistent with previous work incorpor-

Table 2 Particle size and zeta potential of zwitterionic sulfobetaine polymeric micelles at an external phase of PBS pH 6.8 at 37 °C and after 6 h following assembly or after reconstitution from freeze drying. The following conditions are given: fresh polymeric micelles without dye loading; fresh polymeric micelles loaded with the Lumogen Red dye; and polymeric micelles reconstituted following freeze drying

	pH 6.8		Lumogen® loading		Freeze drying	
Code BMA : sulfobetaine	Zeta pot. (mV) Mean (±SD)	Particle size (nm) Mean (PDI)	Zeta pot. (mV) Mean (±SD)	Particle size (nm) Mean (PDI)	Zeta pot. (mV) Mean (±SD)	Particle size (nm) Mean (PDI)
P2S (60 : 40)	−2.13 (±1.59)	28 (0.42)	−1.73 (±2.33)	28 (0.34)	−4.99 (±4.12)	26 (0.31)
P3S (50 : 50)	−1.82 (±1.12)	47 (0.48)	−2.12 (±3.19)	45 (0.46)	−2.78 (±2.52)	46 (0.36)
P4S (40 : 60)	−2.26 (±0.36)	45 (0.43)	−1.31 (±1.20)	43 (0.33)	−3.45 (±2.31)	39 (0.44)
P5S (30 : 70)	−0.57 (±0.06)	49 (0.47)	−2.44 (±1.59)	48 (0.47)	−1.08 (±2.01)	51 (0.48)

ating low concentrations of lipophilic cargo.[72–74] The freeze drying process had little to no impact on both the particle size and zeta potential, supporting that these PMs can be resuspended after freeze drying, if an appropriate cryo-protectant is used; in this study, trehalose was used at a 5 : 1 weight ratio. Trehalose at this weight ratio is reported in many studies to allow successful re-suspension of particles with retention of their original physico-chemical characteristics.[75,76] In addition, the PMs showed no tendency to aggregate when tested over 6 h at both 25 °C and 37 °C after formation. The stability of zwitterionic sulfobetaine PMs against aggregation is due to their highly charged nature where both the quaternary amine and sulfobetaine are totally ionized and do not undergo protonation at any pH value.[77] These highly charged groups at the surface hinder inter-particle interaction.[78,79] Sulfobetaine PMs have shown the required properties in terms of size and surface charge to mimic capsid shell viruses and to potentially display high diffusivity through the intestinal mucus barrier.

3.2.2. Micellar characterization by cryogenic transmission electron microscopy (cryo-TEM). Cryo-TEM was used primarily to characterise the shape of sulfobetaine PMs. While DLS yields average particle sizes that skew towards larger dimensions when compared with TEM, due to the use of dispersants and tendency to form particle aggregation in solution,[80,81] DLS analysis provides a more indicative representation of particle size in solution, as would be experienced with the oral gavage administration of such micellar structures.[82]

For cryo-TEM a single sulfobetaine PM formula was explored (P3S, a BMA : sulfobetaine ratio of 50 : 50). Fig. 2 shows that P3S particles displayed a spherical shape with an average dimension of *ca.* 50 nm. The spherical shape of the sulfobetaine polymers is consistent with that expected from a nanoprecipitation methodology zwitterionic amphiphilic copolymers dispersed in water to form self-assembled micellar structures.[83–85] Typically, block copolymers tend to self-assemble into spherical polymeric micelles when their concentration surpasses the critical micellization concentration (CMC).[86,87] Moreover, the spherical shape of polymeric micelles is attributed in many previous studies to the ratio of hydrophilic-to-hydrophobic components, where block polymers with a hydrophilic mass fraction exceeding 45% tend to form spherical micelles, while those with a lower hydrophilic mass fraction typically self-assemble into vesicles.[88–90] The P3S formula studied by TEM has a hydrophilic block polymer of 50% and all other polymeric micelles in this study are formed from diblock copolymers in which the hydrophilic block is in the range of 40% to 70%.

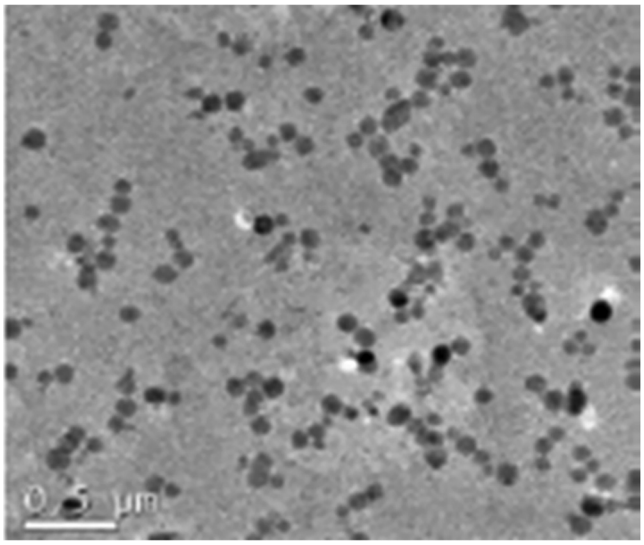

Fig. 2 Cryo-TEM image of the spherical polymeric micelles. Shown is the P3S formulation which is assembled with a hydrophilic sulfobetaine to lipophilic BMA ratio of 50 : 50.

3.3. Diffusion kinetics of sulfobetaine PMs through the native intestinal mucus

The intestinal mucus barrier is a key rate-limiting barrier, preventing nanocarriers from reaching the intestinal absorption surface. Table 3 shows the MPT diffusion data for sulfobetaine PMs (loaded with the Lumogen Red tracking dye) in pig intestinal mucus determined by MPT technology. $\langle D_{eff} \rangle$ is a measure of the absolute diffusion of the PMs through the mucus reflecting both surface chemistry and particle size differences. The respective diffusion of the PMs in water ($D°$) was calculated using the Stokes–Einstein equation and served to account for differences in PMs' particle sizes when considering the particle diffusion in the mucus, *i.e.* it isolates the impact of surface chemistry alone through the % ratio $\langle D_{eff} \rangle / D°$. Table 3 also shows the % diffusive PMs within the mucus. This parameter is inversely reflective of the degree of trapping or slowing of the particle population within the mucus over time; the higher the % the less the contact time of the population (or subpopulation) of any of the particular PM formulations with the mucus components.

Table 3 highlights the diffusion of P3S, P4S and P5S PMs is dependent upon on the ratio of BMA to sulfobetaine, with the zeta potential and particle size showing no positive correlation to either $\langle D_{eff} \rangle$ or % ratio $\langle D_{eff} \rangle / D°$. Statistical analysis ($p < 0.05$) showed that the % ratio $\langle D_{eff} \rangle / D°$ increased significantly with an increase in sulfobetaine content from P2S to P5S. This reflects the influence of the degree of surface charge density providing an overall neutral (or very close to neutral) zeta potential due to the high density of matched +ve and −ve surface charges. Indeed this is the basis of our hypothesis that it is the particles' 'slippery surface properties' rather than the particles' overall surface charge and particle size *per se* that is critical for mucus permeation. This is most clearly exemplified with the P2S formulation (60 : 40 ratio BMA to sulfobetaine) which despite being smaller in size (28 nm), and with a zeta potential not distinctly different to the other PMs, exhibited a $\langle D_{eff} \rangle$ value of approximately 30% lower than the P5S PMs, and a $\langle D_{eff} \rangle / D°$ value 6–7 fold lower.

The relatively high % diffusive PMs (reflecting reduced mucus trapping and slowing of particle diffusion) is seen to

Table 3 Multiple particle tracking (MPT) data for diffusion in the intestinal mucus of sulfobetaine polymeric micelles (PMs) loaded with the Lumogen Red dye. The diffusion coefficient $\langle D_{eff} \rangle$ is a measure of the absolute diffusion of the PMs through the mucus. The respective diffusion of the PMs in water ($D°$) was calculated using the Stokes–Einstein equation. The % ratio $\langle D_{eff} \rangle / D°$ accounts for differences in PMs' particle sizes when considering particle diffusion in the mucus, *i.e.* it isolates the impact of surface chemistry alone. The % of diffusive particles within the mucus is inversely reflective of the degree of trapping or slowing of the particle population within the mucus over time. (N = 3 experiments; mean ± SD). Note: the zeta potential and particle size columns refer to the data as presented in Table 2

Code BMA : sulfobetaine	Zeta potential (mV) Mean (±SD)	Particle size (nm) Mean (PDI)	$D°$ (water) $cm^2\ s^{-1} \times 10^{-9}$	$\langle D_{eff} \rangle$ (mucus) $cm^2\ s^{-1} \times 10^{-9}$ Mean (±SEM)	% ratio $\langle D_{eff} \rangle / D°$	% diffusive particles
P2S (60 : 40)	−1.73 (±2.33)	28 (0.34)	160.50	0.2828 (±0.0768)	0.1762	35
P3S (50 : 50)	−2.12 (±3.19)	45 (0.46)	99.87	0.3447 (±0.0683)	0.3452	44
P4S (40 : 60)	−1.31 (±1.20)	43 (0.33)	99.87	0.5747 (±0.1019)	0.5754	54

increase with a decrease in BMA to sulfobetaine ratio (P2S to P5S), an effect reflecting the increasing shielding of the lipophilic BMA core by the densely charged sulfobetaine external coating (Fig. S3). For PS2, with the highest BMA : sulfobetaine ratio (60 : 40), the lipophilic BMA core is more exposed, increasing the potential for hydrophobic–hydrophobic interactions between the particle and the lipophilic components of the mucus. The shielding of BMA by sulfobetaine is consistent with the work of Lowe *et al.*,[28] who showed that an increase in sulfobetaine to BMA ratio in polymer coated poly(methyl methacrylate) discs increases their anti-adherent properties (antibacterial, anti-macrophage adhesion and dirt resistance).

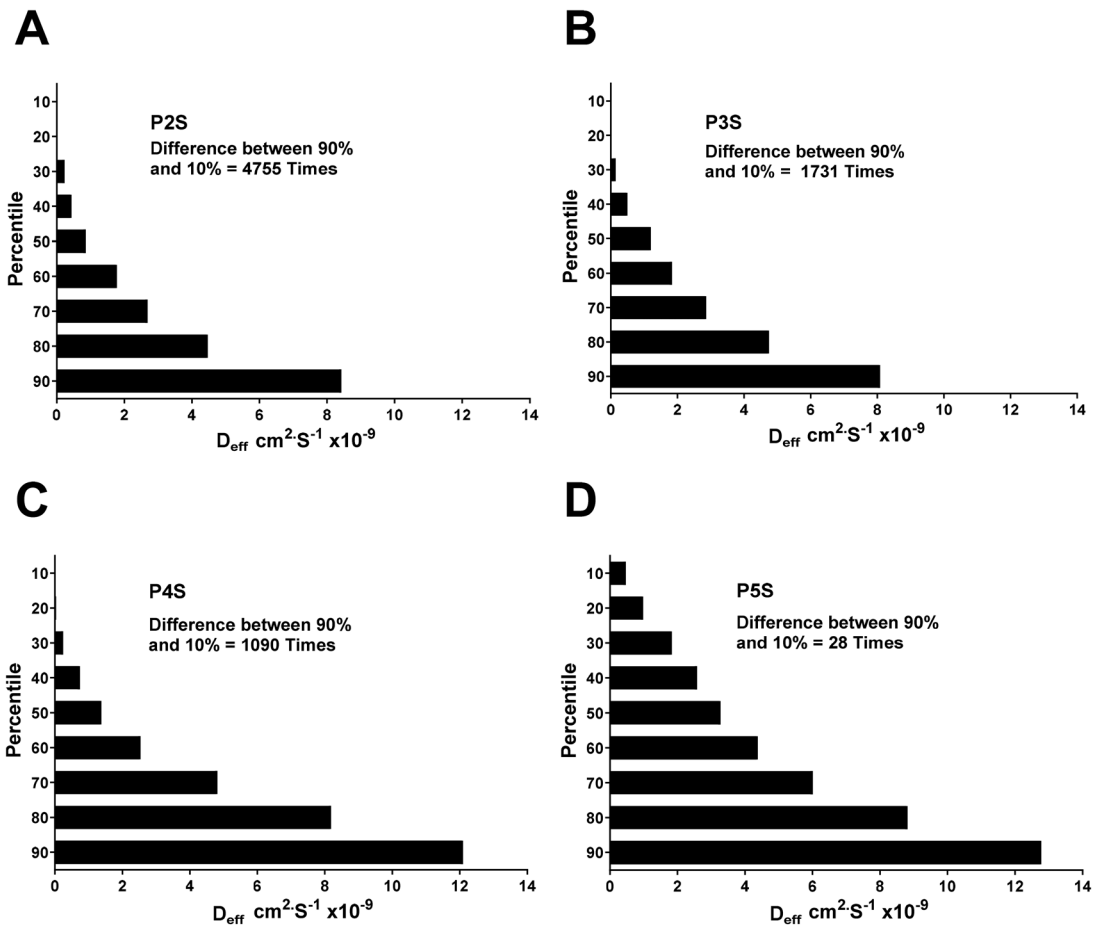

Fig. 3 Intestinal mucus permeation data showing heterogeneity in mucus diffusion for each of the polymer micelle particle formulations – [A] P2S; [B] P3S; [C] P4S; and [D] P5S. For each particle type, an effective diffusion coefficient (D_{eff}) was calculated from 360 individual particles. The data were then ranked into percentiles from the 90th to the 10th. Heterogeneity in (D_{eff}) within the population for a given formulation can be determined by comparing the 90th percentile (fastest particle) to the 10th percentile (slowest particle). The ratio for P5S is 28-fold, P4S is1090-fold, P3S is 1731-fold, and P2S is 4755-fold.

Similar anti-adherent properties of sulfobetaine polymer coatings have been reported.[23,91]

Fig. 3 shows the heterogeneity in mucus diffusion for each of the PM particle formulations expressed as the percentile ranking of ensemble diffusion coefficients $\langle D_{eff} \rangle$. For example, the fastest particles for any formulation are ranked in the 90th percentile, with the P5S PMs in the 90th percentile displaying an ensemble D_{eff} value of 12.7 cm^2 s^{-1} × 10^{-9}. Comparing the D_{eff} values within any PM formulation between the 90th and 10th percentiles shows the heterogeneity in diffusion within that formulation. For the P5S formulation, the 90th (fastest) to 10th (slowest) percentile ratio is 28-fold (Fig. 3D), while the heterogeneity for the other formulations is much greater. For example, for P4S (Fig. 3C) the ratio is 1090-fold, for P3S (Fig. 3B) it is 1731-fold, and for P2S (Fig. 3A) it is 4755-fold. What is apparent is that the heterogeneity in PM diffusion decreases as the BMA to sulfobetaine ratio decreases, *i.e.* a higher content of sulfobetaine to BMA, which results in more uniform and compact distribution of sulfobetaine at the PM surface, facilitating a more homogeneous diffusion within the PM population. Overall, the heterogeneity of the BMA–sulfobetaine PMs is remarkably lower compared to some of our previous studies looking at PMs with varying hydrophilic surface properties.[32] The BMA–sulfobetaine PMs also show, in general, a high diffusion rate, *e.g.* for the context using the same MPT technique, PLGA NPs show a $\langle D_{eff} \rangle / D^{\circ}$ ratio of 0.0005 (ref. 32) compared to 1.1895 for P5S in this study (2300-fold higher diffusivity). This MPT diffusion in the intestinal mucus indicates the slippery properties of sulfobetaine PMs and highly supports the hypothesis that sulfobetaine PMs can improve the bioavailability of loaded peptides through efficient permeation across the intestinal mucus barrier.

3.4. Cytotoxicity of sulfobetaine PMs

The cytotoxicity of sulfobetaine PMs was examined in two epithelial cell models (MDCK-II and Caco-2 cell lines) using an

Table 4 Ion pairing molar ratios of SDS with exenatide and the resulting % of exenatide–dodecylsulphate yield at pH 4.0 and pH 3.0. The SDS : exenatide molar ratio of 4 : 1 at pH 4.0 was used to synthesise P5S PM formulations through *in vivo* experiments

Molar concentration ratio (SDS : exenatide)	Media pH 4.0 % yield of exenatide dodecylsulphate	Media pH 3.0 % yield of exenatide dodecylsulphate
3 : 1	85.99 (±1.66)	79.68 (±5.78)
4 : 1	88.47 (±0.29)	81.68 (±2.69)
5 : 1	82.77 (±4.31)	80.94 (±2.35)

Table 5 Entrapment efficiency (EE%) and loading capacity (LD%) of sulfobetaine polymeric micelles, where the loading of exenatide dodecylsulphate was performed at pH 4.0 (N = 3; mean ± S.D.)

Code BMA : sulfobetaine	Entrapment efficiency (%) (±SD)	Loading capacity (%) (LD%) (±SD)
P2S (60 : 40)	90.51 (±0.74)	13.58 (±0.11)
P3S (50 : 50)	92.07 (±0.86)	13.81 (±0.13)
P4S (40 : 60)	94.87 (±0.52)	14.23 (±0.78)
P5S (30 : 70)	96.46 (±0.26)	14.47 (±0.04)

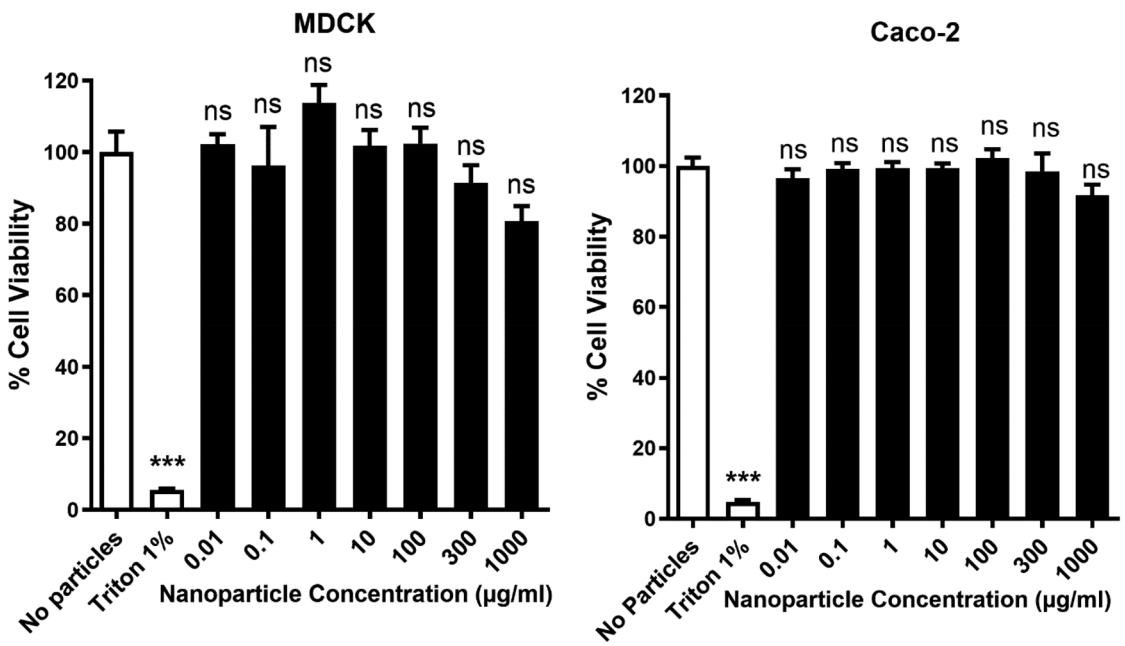

Fig. 4 *In vitro* cytotoxicity study of the P5S polymeric sulfobetaine polymeric micelles against the renal epithelial cell line, MDCKII, and the intestinal epithelial cell line, Caco-2. The cells were exposed to the P5S sulfobetaine PMs for 24 h at the concentrations shown. The no particle treatment was the negative control while 1% Triton treatment was the positive control. Data represent the mean ± SEM of three experiments (N = 3). ns: no significant difference compared to the negative control group.

MTT viability assay. Fig. 4 shows the viability of cells in response to a range of PM concentrations (0.01 μg ml^{-1} to 1000 μg ml^{-1}) compared to the no-particle negative control (100% viability) and the positive control of 1% Triton (0% viability). The maximum polymeric PM concentration (1 mg ml^{-1}) selected for these *in vitro* viability studies reflects the indicative maximum possible concentration such that the PMs can reach the lumen of the gastrointestinal tract following oral gavage administration of a 1 ml volume containing a 1 mg dose of PMs loaded with exenatide (this work's *in vivo* study). Fig. 4 shows for both MDCKII and Caco-2 cells no significant difference in cell viability across all the concentrations of PMs, compared to the negative control's 100% viability arm. This provides encouraging evidence that sulfobetaine PMs are non-toxic toward at least these renal and intestinal epithelial cell models. This finding is in agreement with previous cytotoxicity studies on sulfobetaine polymers, where no evidence was found in both *in vitro*[92,93] and *in vivo*[94] cytotoxicity tests.

3.5. Oral delivery of exenatide from sulfobetaine PMs

3.5.1. Loading of exenatide into sulfobetaine PMs. The strategy involved loading exenatide into the lipophilic core (BMA core) of the sulfobetaine PMs. In this manner, avoiding the rapid 'burst release' of exenatide from the PM surface while also providing greater protection of the peptide from catalytic and enzymatic environments, *e.g.* acid conditions of the stomach.[95] Loading to the core also facilitated a more sustained release profile.[16,96] To enable this loading approach to the hydrophobic core, exenatide was ion-paired with SDS, producing a lipophilic entity, exenatide–dodecylsulphate.

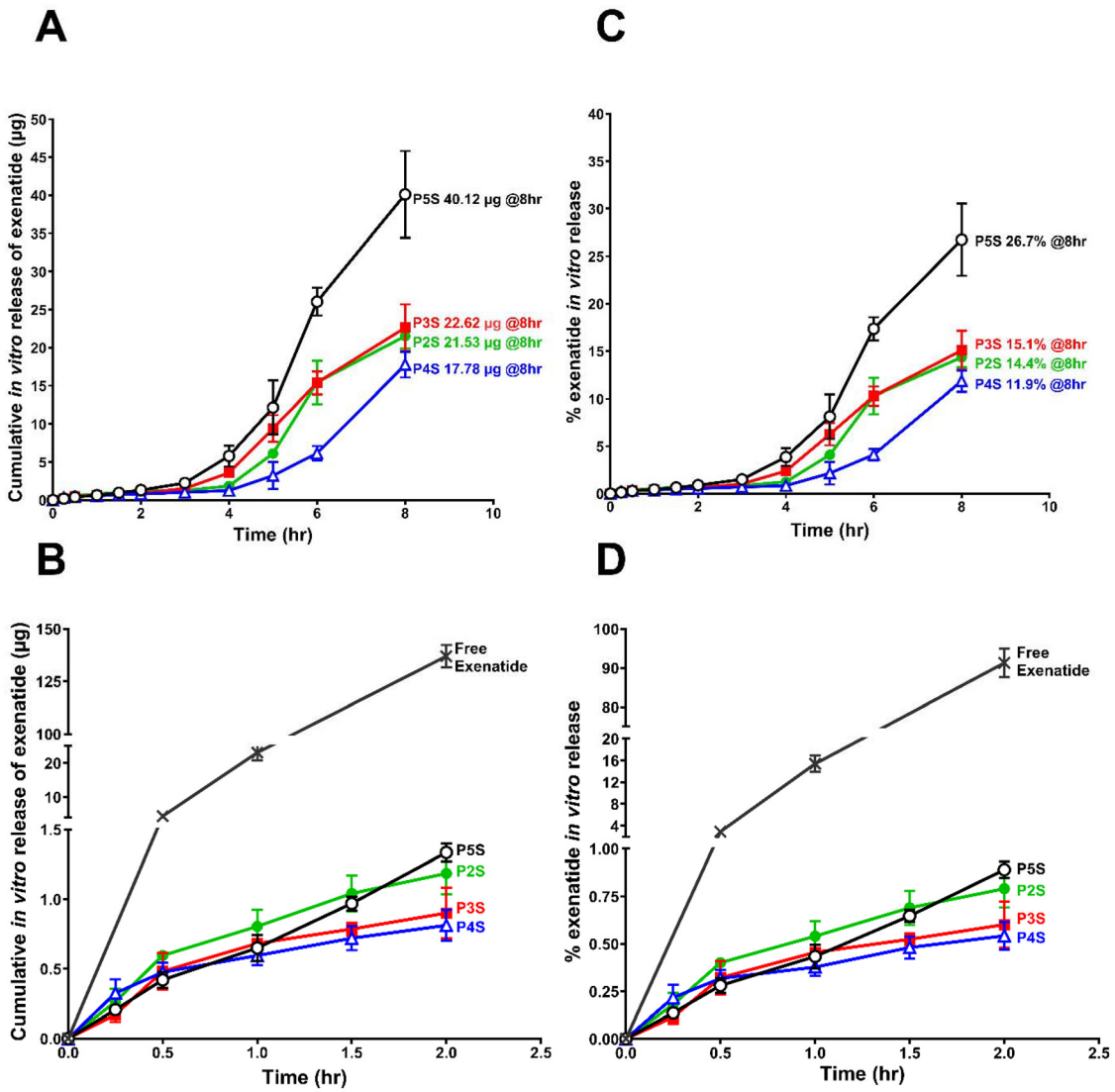

Fig. 5 Cumulative release profiles of exenatide from the polymeric micelles (designated P2S to P5S) in pH 6.8 buffer. [A] mass (μg) release profile through 0 to 8 h; [B] mass (μg) release profile in the first 0 to 2 h alone. Also shown is the transfer of free exenatide across the dialysis tubing over the same first 2 h (the recovery of which was 95%). [C] and [D] show the corresponding % release data. An equivalent of 150 μg of exenatide represented the starting mass for each of the release profiles. Data represent the mean ± SD of three experiments (N = 3).

Exenatide is a 39 amino acid hydrophilic peptide (MW = 4186.6 g mol^{-1}) with four basic amino acids and an isoelectric point of 4.86.[97] At low pH, these four basic amino acid units (*i.e.* H_1, R_{20}, K_{12}, and K_{27}) are positively charged enabling the ion pairing of the peptide with a negatively charged surfactant.[98] Exenatide and SDS were mixed at two different buffer solutions (pH 4.0 and pH 3.0) to drive the ionisation of exenatide. As shown in Table 4, ion pairing with SDS at a molar ratio of 4 : 1 (SDS to exenatide) at pH 4.0 leads to the highest % exenatide–dodecylsulphate yield (88.47%, ±0.29); these conditions were then used to synthesise P5S PM formulations for *in vivo* experiments. While the lower pH of 3.0 may have been expected to achieve a higher yield (slightly higher ionisation of exenatide), this was consistently not evidenced in the preliminary studies and may reflect some minor conformational restrictions at pH 3.0, not conducive to a higher ion-pairing outcome. The lipophilic exenatide–dodecylsulphate was then loaded into the sulfobetaine PMs, and Table 5 shows the resulting entrapment efficiency (EE%; eqn (3)) and loading capacity (LD%; eqn (4)). An EE% exceeding 90% and an LD% exceeding 13.5% represent a loading level more than acceptable for pharmaceutical uses.[99]

3.5.2. *In vitro* release of exenatide from sulfobetaine PMs and further particle characterisation in acid/pepsin. Here we first explored the release kinetics of the exenatide peptide from the sulfobetaine PM particles under pH 6.8 and pH 1.2 conditions. Fig. 5A and B show cumulative mass (μg) release profiles of exenatide from the PMs through a dialysis membrane in a pH 6.8 buffer. Fig. 5A shows the profile across an entire 0 to 8 h release experiment, while Fig. 5B shows the 0 to 2 h profile alone, as well as the transfer of free exenatide (*i.e.* free in solution and not from a particle) across the dialysis

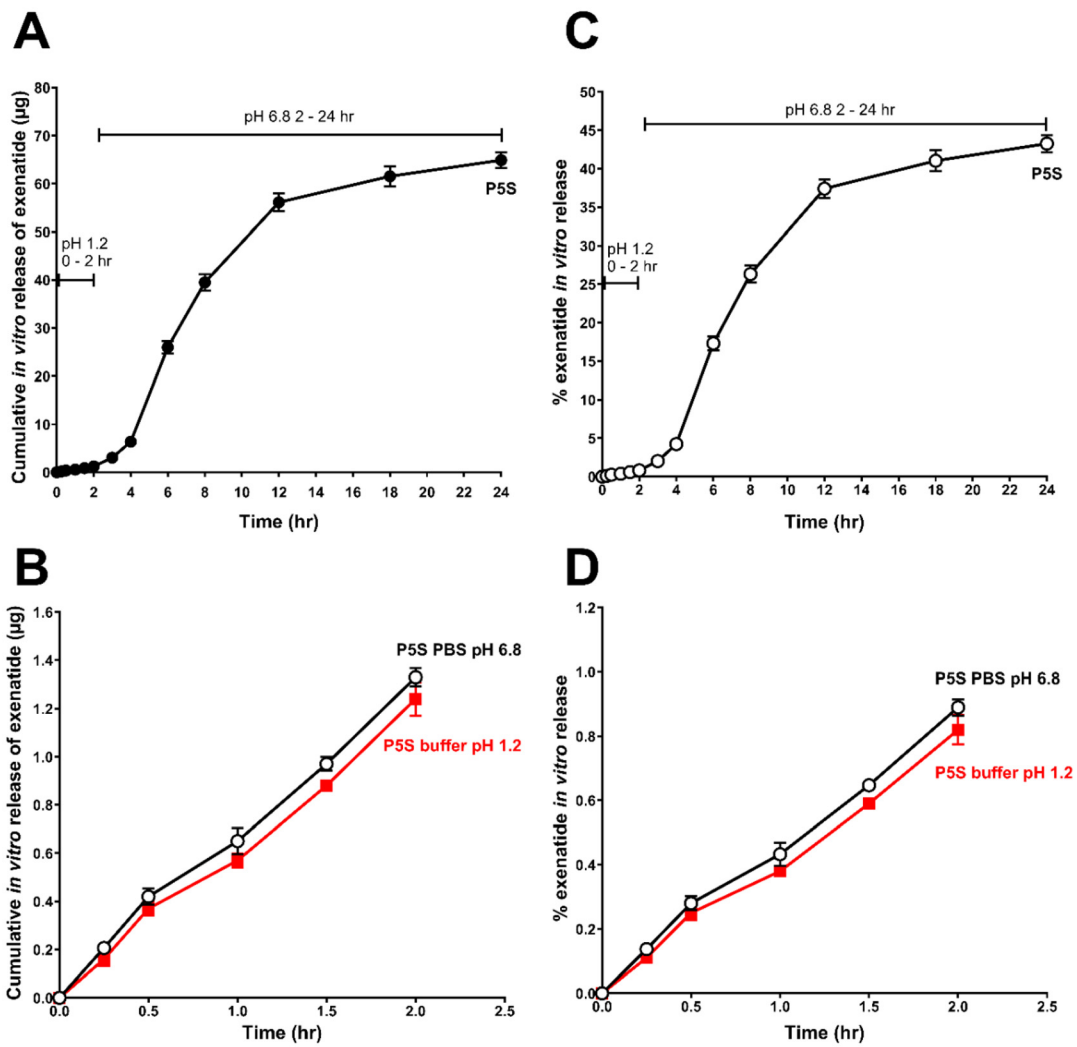

Fig. 6 Cumulative release profile of exenatide from the P5S polymeric micelle formulation. [A] mass (μg) release over 24 h, where the first 0 to 2 h of studies were conducted at pH 1.2 and the remaining 2 to 24 h at pH 6.8. [B] mass (μg) release in the first 0 to 2 h comparing two buffer conditions of pH 1.2 and pH 6.8 and which show no significant difference (NS) in exenatide release between these two different pH media. [C] and [D] show the corresponding % release data. An equivalent of 150 μg of exenatide represented the starting mass for each of the release profiles. Data represent the mean ± SD of three experiments (N = 3).

tubing over the same first 2 h, and which showed 95% dose recovery. Fig. 5C and D show the respective % release data. An equivalent exenatide mass of 150 μg represented the starting mass for each of the PM release profiles, as indeed the starting mass for the free exenatide.

The overall release rates from the PMs over the first 8 h averaged for P2S, 2.69 μg h^{-1}; PS3, 2.83 μg h^{-1}; PS4, 2.22 μg h^{-1}; and PS5 5.02 μg h^{-1}. While the release rates over the more linear pseudo-steady-state component of the profiles (4 h to 8 h) were PS2, 4.92 μg h^{-1}; P3S, 4.76 μg h^{-1}; P4S, 4.13 μg h^{-1}; and P5S, 5.58 μg h^{-1}. By 8 h the formulations P4S, P2S and P3S had released 17.78, 21.53 and 22.62 μg of exenatide representing 11.9% to 15.1% of the loaded dose (Fig. 5C). In all cases the PM formulation with the smallest BMA hydrophobic core, P5S, showed the greatest rate of release and the greatest mass released, with 40.12 μg of exenatide released from P5S by 8 h, *i.e.* 26.7% of the load. The faster release of exenatide from the P5S particles attributed to the swelling and dissolution of the exterior hydrophilic surface and diffusion of the drug into the external media.[100,101] The P5S sulfobetaine polymeric micelles exhibit the highest hydrophilic component (BMA : sulfobetaine (30 : 70) ratio), which leads to faster swelling and dissolution of the hydrophilic shell and faster drug diffusion into the external media.[102]

This initial experiment determined which sulfobetaine particle to take forward for further *in vitro* release charactersation and for *in vivo* experimentation, P5S. It also provided assurance that the exenatide release from the PMs was not significantly due to a surface 'burst' phenomenon, but rather sustained release from the PM interior; an important efficiency and protective consideration if the peptide-containing PMs were to reach the absorption surface below the intestinal mucus barrier and still retaining the vast majority of their cargo.[16,103,104]

We next explored the impact of acid and pepsin exposure over a 2 h period (37 °C) upon particle characteristics and found no meaningful impact. In PBS buffer pH 7.2, the P5S sulfobetaine PMs' particle size was 45 nm (PDI 0.38), and with pepsin at pH 7.2, the particle size was 47 nm (PDI 0.48). A slight increase in polydispersity was noted but nevertheless it remains very similar between the conditions and close that reported in Table 2. As pepsin is not activated at neutral pH, this result is as predicted. At pH 1.2 in the absence of pepsin the particle size was 54 nm (PDI 0.39) with the addition of pepsin under these acidic conditions resulting in a particle size of 50 nm (PDI 0.47). Again the data were similar in the presence and absence of pepsin, again perhaps not surprising as the polymer chemistry of these particles is not the one constituted by peptide bonds. If anything, the low acidic pH conditions and no pepsin activation *per se* showed a marginal tendency for slightly larger particle size measurements (45 nm *vs.* 54 nm for the pH 7.2 and pH 1.2 conditions, respectively). The PDIs reported for the P5S polymeric micelles under all conditions in the work were between 0.38 and 0.48. The distribution pattern in the size *vs.* intensity plots excluded the generation of smaller more dispersed particles. Incubation of the particles at pH 1.2 (whether pepsin was present or not) showed a zeta potential decrease to −5.0 mV from that observed at a neutral pH value of −1.0 to −2.0 mV. This was reversible when the particles were returned to neutral pH. These data support that low pH conditions and the presence of pepsin did not have a profound effect on the structural integrity of our particles. As such we may consider that our particles, to a large extent, would preserve the integrity (against a low pH value and pepsin) of any peptide cargo within the inner core of the P5S sulfobetaine particles.

Next we undertook a more prolonged 24 h extended release study using P5S, and the first 2 h studies were conducted under either acidic (pH 1.2 buffer; KCL, HCL) or near to neutral (pH 6.8 buffer; PBS) conditions. After that the same PM formulations were transferred to a fresh pH 6.8 buffer for the remaining 22 h (*i.e.* between 2 h and 24 h post the start of the release study). Fig. 6 shows the extended release profile for P5S with 6A and 6B showing the cumulative mass (μg) release profiles of exenatide, respectively, across the entire 0 to 24 h experiment and then just the initial 0 to 2 h. Fig. 6C and D show the respective % release data. Release from the P5S PM formulation in this more extended study was similar to that seen in earlier work (Fig. 5), with the lag phase up to 4 h prior to the more linear pseudo-steady-state release. By 8 h some 40 μg of exenatide (26%) had been released. By 24 h a mass of 65 μg (43%) had been released, an extent of mass release likely necessary for *in vivo* experimentation.[105] During the first 2 h (Fig. 6B and D) the release was less than 1.4 μg (less than 0.9%) and was not impacted by the very less acidic conditions

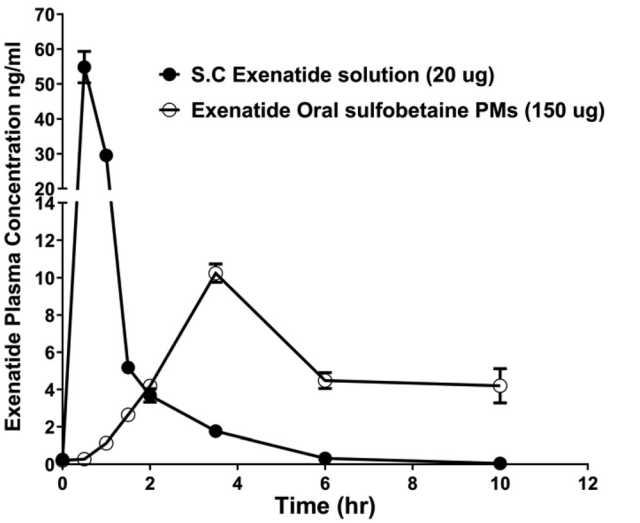

Fig. 7 Exenatide plasma concentration–time profiles for the s.c. administered exenatide solution (exenatide dose of 20 μg) and the orally administered P5S exenatide–sulfobetaine polymeric micelles (PMs) (exenatide dose of 150 μg). The levels of exenatide following the oral administration of exenatide as a solution were undetectable at all timepoints. The area under the curve (AUC) calculated from the observed data (0 to 10 h) averaged for s.c. exenatide is 53.2 ng ml^{-1} h, while the comparative AUC (0 to 10 h) for orally administered exenatide–sulfobetaine PMs averaged 49.7 ng ml^{-1} h. Data represent the mean ± S.E.M (N = 3).

(pH 1.2). These results directly coincide with the conclusions from the above particle characterisation work, *i.e.* particles can be exposed to less acidic conditions and remain stable in order to release peptide cargo at the same rate as that seen at neutral pH. Ultimately of course, if the acid or pepsin environment of the stomach was found to be detrimental to the effective oral delivery of peptides using sulfobetaine polymeric micelle particles (which is not evidenced by the *in vivo* data we present below), then a final polymeric micelle formulation could be incorporated into enteric capsules.

3.6. PK–PD *in vivo* efficacy in a rodent model

The PK studies followed the exenatide level for 10 h (four times the elimination half-life of exenatide which is *ca.* 2.4 h). Fig. 7 shows exenatide plasma concentration–time profiles for the s.c. administered exenatide solution (exenatide dose of 20 μg) and the orally administered P5S exenatide–sulfobetaine PMs (exenatide dose of 150 μg). The levels of exenatide following the oral administration as an exenatide solution were undetectable, indicating total degradation in the gastro-intesti-

Table 6 PK variables in the rats comparing the subcutaneous (s.c.) administration of exenatide solution (dose 20 μg) to the oral administration of exenatide (dose 150 μg) encapsulated into P5S sulfobetaine polymeric micelle (PM) nanoparticles (N = 3; mean ± SEM)

PK variable for exenatide	Subcutaneous solution (20 μg)	Oral sulfobetaine PM nanoparticles (150 μg)
C_{max} (ng ml^{-1}) (observed)	54.8 (±5.6)	10.2 (±0.63)
T_{max} (h) (observed)	0.50	3.5
$AUC_{(0–10\ h)}$ (ng ml^{-1} h)	53.2 (±38.4)	49.7 (±45.1)
$C_{last_{(10\ h)}}$ (ng ml^{-1}) (measured)	<0.20	4.30 (±1.12)
Relative extent of bioavailability for exenatide from the oral polymeric micelles (*versus* s.c. route) (%)	N/A	13.0 (±2.16)

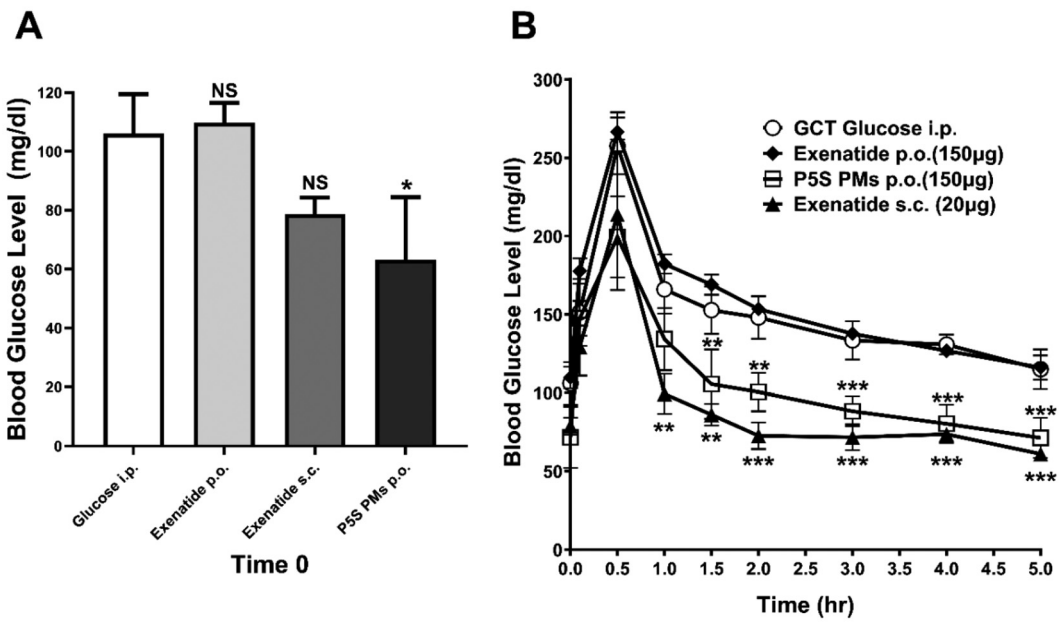

Fig. 8 The PD study based on the measurement of blood glucose levels in response to a glucose challenge test (i.p. GCT 'no treatment' control). The exenatide treatments always preceded the i.p. glucose (GCT) administations. For each individual formulation, the time period following exenatide administration prior to the i.p. GCT was optimised so as to correspond to peak (near-peak) exenatide plasma levels at the point of i.p. GCT administration; for s.c. exenatide this was 10 min, while for oral solution exenatide (*Exenatide p.o.*) and for the sulfobetaine poylmeric micelles (*P5S PMs p.o.*) this was 4 h. [A] Endogenous glucose levels at time zero immediately before i.p. glucose administration. The orally administered exenatide–sulfobetaine PMs (administered 4 h previously) reduced endogenous blood glucose levels significantly greater than any other treatment arms. [B] Blood glucose levels following the i.p. glucose challenge test for the treatments. Exenatide oral solution (*Exenatide p.o. 150 μg*) given 4 h before the i.p. GCT showed no effect on the glucose levels. Exenatide delivered orally by P5S sulfobetaine PMs (*P5S PMs p.o. 150 μg*) showed a significant decrease in glucose levels throughout the 1.5 h to 5 h post-GCT period. Similarly, s.c. exenatide solution (*Exenatide s.c. 20 μg*) significantly reduced blood glucose levels over the 1 h to 5 h post-GCT period. From 0.5 h to 5 h post-GCT challenge no statistical differences were observed between the glucose levels in the oral exenatide–sulfobetaine PMs and the s.c. exenatide solution administration. Data represent the mean ± SD (N = 4 or each glucose time profile). Statistically significant differences were observed (**P < 0.01), (*** ≤ 0.001) when comparing data with those of the glucose challenge test alone (glucose i.p.).

nal lumen. This has been observed previously for oral exenatide solution.[106,107]

Table 6 shows some of the PK parameter variables for exenatide. The s.c. administration of exenatide solution reached its maximum observed concentration of 54.8 ng ml^{-1} at 0.5 h (similar to that reported by others[105–109]) with the levels then reducing to essentially zero by 10 h. The exenatide delivered *via* oral sulfobetaine PMs reached a maximum observed concentration of 10.2 ng ml^{-1} at 3.5 h after administration, followed by slower decline with extended plasma levels of up to 10 h (C_{last} 4.30 ng ml^{-1}) and beyond. This extended plasma profile is consistent with the slower release profile of exenatide from sulfobetaine PMs and the rat gastric emptying, which will delay, to some extent, the PMs reaching the intestinal absorption site.[110,111] The area under the curve ($AUC_{(0–10\ h)}$) calculated from the observed first 10 h data alone was, for s.c. exenatide, 53.2 ng ml^{-1} h, while for exenatide delivered orally *via* sulfobetaine PMs, it was 49.7 ng ml^{-1} h. From the $AUC_{(0–10\ h)}$ alone we determined the relative bioavailability of the orally administered exenatide PMs at 13% compared to the s.c. solution administration. This indicates efficient protection of the loaded peptide and the high mucus permeability of sulfobetaine PMs, at least with respect to this non-clinical model.

The PD study was based on the measurement of blood glucose levels in response to a glucose challenge test (i.p. GCT),[112] the glucose challenge test having first been preceded where appropriate by exenatide administrations. For each individual formulation the time period following exenatide administration prior to the i.p. GCT was optimised so as to correspond to peak (near-peak) exenatide plasma levels at the point of i.p. GCT administration; for s.c. exenatide this was 10 min, while for oral solution exenatide (*Exenatide p.o.*) and for the sulfobetaine poylmeric micelles (*P5S PMs p.o.*) this was 4 h. Measuring blood glucose levels following the GCT in this way also allow the assessment of pharmacodynamic equivalencies between the various administrations.[113]

Fig. 8A shows the endogenous glucose levels at time zero immediately before i.p. glucose administration. The orally administered exenatide–sulfobetaine PMs (administered 4 h previously reduced endogenous blood glucose levels significantly greater than any other treatment arms (Fig. 8A). Fig. 8B shows the blood glucose level profiles for the various administrations at times 0, 0.16, 0.5, 1, 1.5, 2, 3, 4 and 5 h following the GCT (glucose i.p. administration); again time 0 refers to the timepoint immediately before i.p. glucose challenge). Exenatide oral solution (*Exenatide p.o. 150 μg*) given 4 h before the GCT showed no effect on the glucose levels, compared with the control GCT arm alone. This is not surprising since the PK study confirmed that there was no evidence of systemic exenatide levels following this solution dose administration. In contrast, exenatide delivered orally by P5S sulfobetaine PMs (*P5S PMs p.o. 150 μg*) showed a significant decrease in glucose levels throughout the 1.5 h to 5 h post GCT period. Similarly, s.c. exenatide solution (*Exenatide s.c. 20 μg*) significantly reduced blood glucose levels over the 1 h to 5 h post GCT period. From 0.5 h to 5 h post GCT challenge there were no statistical differences between the glucose levels in the oral exenatide–sulfobetaine PMs and the s.c. exenatide solution administrations. Over the period the PD data would also support a relative PD bioequivalence estimate for the exenatide–sulfobetaine PMs (relative to the s.c. administration) of at least 13%, *i.e.* considering the glucose response profiles to be similar between s.c. and oral exenatide–sulfobetaine PM treatments but the oral PMs requiring a 7.5-fold higher dose to that of the s.c. administration.

4. Conclusion

In this study, novel highly charged zwitterionic sulfobetaine polymeric micelles (PMs) were designed and synthesised using RAFT polymerisation. These PMs have not been previously reported in terms of a biological application as mucus-diffusive particles for oral peptide delivery. The study showed the production of uniformly reproducible BMA–sulfobetaine PMs of small sizes (<50 nm) and with hydrophobic and hydrophilic components precisely tuneable as needed to accommodate different cargoes. These sulfobetaine PMs mimic the surface chemistry of capsid viruses with a highly densely charged but overall neutral surface. They efficiently permeate rate-limiting intestinal mucus layers, showing a direct correlation between diffusivity through the mucus and the degree of the hydrophilicity of the outer shell coating. The sulfobetaine PMs are likely to facilitate the oral delivery of the loaded peptide, at least to some extent, *via* their enhanced ability to permeate the mucus and hence achieve close proximity to the intestinal epithelial absorption surface.

These PMs were shown to exhibit a high capacity to load a hydrophilic model peptide, exenatide, into the PMs' hydrophobic core, achieved by an ion-pairing strategy. In *in vitro* release studies they provided for a controlled and substantive release of peptides over 24 h. They are resistant to the effects of very low pH acidic (and pepsin-containing) environments and do not display cytotoxicity in standard cell epithelial viability assays. An *in vivo* PK–PD study in rats demonstrated the oral delivery of exenatide-loaded sulfobetaine polymeric micelles to achieve a relative extent of peptide bioavailability of 13% compared to a subcutaneous (s.c.) exenatide solution injection. This favourable PK outcome was paralleled in PD studies addressing the efficacy of oral delivery of exenatide-loaded sulfobetaine polymeric micelles to reduce blood glucose levels following a glucose challenge. This polymeric micelle technology has very real potential for oral peptide delivery including the delivery of GLP-1 agents,[15] which are of intense therapeutic interest at present. Based on the above, this novel family of stable sulfobetaine polymeric micelles are promising tools to further explore the oral peptide delivery, and in particular with respect to the high capacity of these micelles to permeate the intestinal mucus barrier. Clearly, while the mucus permeation and PK and PD outcomes have been the key foci of this work, future studies will need to

explore in detail the interaction of these particles with the intestinal epithelium itself.

Author contributions

Muthanna Abdulkarim: conceptualisation, methodology, validation, investigation, funding acquisition, analysis, and writing – original draft. Flavia Laffleur: methodology and reviewing. Victor Ramos-Pérez: methodology. Andreas Bernkop-Schnürch: conceptualization, reviewing and editing, and funding acquisition. Salvador Gómez Borros: conceptualization, and reviewing and editing. Catia Neto: methodology, validation, investigation, and analysis. Mark Gumbleton: conceptualization, methodology, validation, funding acquisition, and writing – review and editing.

Conflicts of interest

The authors have no conflicts to declare.

Abbreviations

AUC	Area under the curve
AIBN	2,2′-Azobis(2-methylpropionitrile)
BMA	Butyl methacrylate
CTA	2-Cyano-2-propyl dodecyl tri-thiocarbonate
D_{eff}	Diffusion coefficient
$\langle D_{eff} \rangle$	Ensemble diffusion coefficient
DMAEMA	Dimethyl aminoethyl methacrylate
DMEM	Dulbecco's modified Eagle's medium
EE%	Entrapment efficiency
FBS	Fetal bovine serum
GCT	Glucose challenge test
GIT	Gastrointestinal tract
GLP-1	Glucagon-like peptide 1
GPC	Gel permeation chromatography
i.p.	Intraperitoneal
LD%	Loading capacity
LLQ	Lower limit of quantification
MDCK-II cells	Madin–Darby canine kidney cells
MTT	3-[4,5-Dimethylthiazol-2-yl]-2,5-diphenyl-tetrazolium bromide salt
M_{n_a}	Number average MW
ns	Not significant
MPT	Multiple particle tracking
MSD	Mean squared displacement
⟨MSD⟩	Ensemble mean squared displacement
MW	Molecular weight
M_{w_a}	Average weight MW
MWCO	Molecular weight cut-off
PD	Pharmacodynamic
PDI	Polymer polydispersity index
PM	Polymeric micelles
Pg	Pico gram
PK	Pharmacokinetic
RAFT	Reversible addition fragmentation chain transfer
s	Second
s.c.	Subcutaneous
SDS	Sodium dodecylsulphate
T2D	Type 2 diabetes mellitus
THF	Tetrahydrofuran

Data availability

All data supporting the findings of this study are available within the SI. Researchers interested in accessing the data for further analysis or verification can refer to the SI.

For any additional inquiries regarding the data, please contact the corresponding author.

Supplementary information: supplementary files, figures, and tables. See DOI: https://doi.org/10.1039/d4pm00202d.

Acknowledgements

The polymer synthesis, PM formation and characterisation studies were financially supported by the EU-project ALEXANDER (Mucosal nanoparticulate delivery systems for macromolecular drugs – Grant agreement ID: 280761). The study of the oral delivery of peptides, including animal studies, was funded by the Welsh government grant LSBF/R3-009 (mucus permeating nanocarriers for oral peptide delivery).

References

1 M. R. Knowles and R. C. Boucher, Mucus clearance as a primary innate defense mechanism for mammalian airways, *J. Clin. Invest.*, 2002, **109**, 571–577.
2 S. K. Linden, P. Sutton, N. G. Karlsson, V. Korolik and M. a McGuckin, Mucins in the mucosal barrier to infection, *Mucosal Immunol.*, 2008, **1**, 183–197.
3 J. D. Kaunitz, Barrier function of gastric mucus, *Keio J. Med.*, 1999, **48**, 63–68.
4 R. A. Cone, Barrier properties of mucus, *Adv. Drug Delivery Rev.*, 2009, **61**, 75–85.
5 A. W. Larhed, P. Artursson and E. Björk, *Pharm. Res.*, 1998, **15**, 66–71.
6 S. C. Bischoff, G. Barbara, W. Buurman, T. Ockhuizen, J.-D. Schulzke, M. Serino, H. Tilg, A. Watson and J. Wells, Intestinal permeability ¿ a new target for disease prevention and therapy, *BMC Gastroenterol.*, 2014, **14**, 189–214.
7 J. L. Lau and M. K. Dunn, Therapeutic peptides: Historical perspectives, current development trends, and future directions, *Bioorg. Med. Chem.*, 2018, **26**, 2700–2707.
8 A. C. L. Lee, J. L. Harris, K. K. Khanna and J. H. Hong, A comprehensive review on current advances in peptide

drug development and design, *Int. J. Mol. Sci.*, 2019, **20**, 1–21.
9 R. B. Shah, M. Patel, D. M. Maahs and V. N. Shah, Insulin delivery methods: Past, present and future, *Int. J. Pharm. Invest.*, 2016, **6**, 1–9.
10 A. Mullard, Once-yearly device takes on daily and weekly diabetes drugs, *Nat. Biotechnol.*, 2014, **32**, 1178.
11 L. M. Neff and R. F. Kushner, Emerging role of GLP-1 receptor agonists in the treatment of obesity, *Diabetes Metab. Syndr. Obes.*, 2010, 263–273.
12 L. Van Bloemendaal, R. G. Ijzerman, J. S. Ten Kulve, F. Barkhof, R. J. Konrad, M. L. Drent, D. J. Veltman and M. Diamant, GLP-1 receptor activation modulates appetite- and reward-related brain areas in humans, *Diabetes*, 2014, **63**, 4186–4196.
13 J. J. Meier, Efficacy of Semaglutide in a Subcutaneous and an Oral Formulation, *Front. Endocrinol.*, 2021, **12**, 645617.
14 A. Andersen, F. K. Knop and T. Vilsbøll, A Pharmacological and Clinical Overview of Oral Semaglutide for the Treatment of Type 2 Diabetes, *Drugs*, 2021, **81**, 1003–1030.
15 FDA, *RYBELSUS (semaglutide) tablets*, 2017.
16 A. des Rieux, V. Fievez, M. Garinot, Y. J. Schneider and V. Préat, Nanoparticles as potential oral delivery systems of proteins and vaccines: A mechanistic approach, *J. Controlled Release*, 2006, **116**, 1–27.
17 T. Jung, W. Kamm, A. Breitenbach, E. Kaiserling, J. X. Xiao and T. Kissel, Biodegradable nanoparticles for oral delivery of peptides: Is there a role for polymers to affect mucosal uptake?, *Eur. J. Pharm. Biopharm.*, 2000, **50**, 147–160.
18 S. K. Lai, D. E. O'Hanlon, S. Harrold, S. T. Man, Y.-Y. Wang, R. Cone and J. Hanes, Rapid transport of large polymeric nanoparticles in fresh undiluted human mucus, *Proc. Natl. Acad. Sci. U. S. A.*, 2007, **104**, 1482–1487.
19 S. S. Olmsted, J. L. Padgett, A. I. Yudin, K. J. Whaley, T. R. Moench and R. A. Cone, Diffusion of macromolecules and virus-like particles in human cervical mucus, *Biophys. J.*, 2001, **81**, 1930–1937.
20 A. B. Lowe and C. L. McCormick, Stimuli responsive water soluble and amphiphilic (co)polymers, *ACS Symp. Ser.*, 2001, **780**, 1–13.
21 N. Tarannum and M. Singh, Advances in Synthesis and Applications of Sulfo and Carbo Analogues of Polybetaines: A Review, *Rev. Adv. Sci. Eng.*, 2013, **2**, 90–111.
22 X. Peng, L. Zhao, G. Du, X. Wei, J. Guo, X. Wang, G. Guo and Q. Pu, Charge tunable zwitterionic polyampholyte layers formed in cyclic olefin copolymer microchannels through photochemical graft polymerization, *ACS Appl. Mater. Interfaces*, 2013, **5**, 1017–1023.
23 Q. Li, H.-H. Lin and X.-L. Wang, Preparation of Sulfobetaine-Grafted PVDF Hollow Fiber Membranes with a Stably Anti-Protein-Fouling Performance, *Membranes*, 2014, **4**, 181–199.
24 X. Han, Y. Lu, J. Xie, E. Zhang, H. Zhu, H. Du, K. Wang, B. Song, C. Yang, Y. Shi and Z. Cao, Zwitterionic micelles efficiently deliver oral insulin without opening tight junctions, *Nat. Nanotechnol.*, 2020, **15**, 605–614.
25 Y. Li, W. Ji, H. Peng, R. Zhao, T. Zhang, Z. Lu, J. Yang, R. Liu and X. Zhang, Charge-switchable zwitterionic polycarboxybetaine particle as an intestinal permeation enhancer for efficient oral insulin delivery, *Theranostics*, 2021, **11**, 4452–4466.
26 D. J. Keddie, A guide to the synthesis of block copolymers using reversible-addition fragmentation chain transfer (RAFT) polymerization, *Chem. Soc. Rev.*, 2013, **43**, 496–505.
27 J. Pretula, K. Kaluzynski, B. Wisniewski, R. Szymanski, T. Loontjens and S. Penczek, Formation of poly(ethylene phosphates) in polycondensation of H3PO4 with ethylene glycol. Kinetic and mechanistic study, *J. Polym. Sci., Part A: Polym. Chem.*, 2008, **46**, 830–843.
28 A. B. Lowe, M. Vamvakaki, M. a. Wassall, L. Wong, N. C. Billingham, S. P. Armes and A. W. Lloyd, Well-defined sulfobetaine-based statistical copolymers as potential antibioadherent coatings, *J. Biomed. Mater. Res.*, 2000, **52**, 88–94.
29 K. S. Yadav and K. K. Sawant, Modified nanoprecipitation method for preparation of cytarabine-loaded PLGA nanoparticles, *AAPS PharmSciTech*, 2010, **11**, 1456–1465.
30 M. Sameti, G. Bohr, M. N. V. Ravi Kumar, C. Kneuer, U. Bakowsky, M. Nacken, H. Schmidt and C. M. Lehr, Stabilisation by freeze-drying of cationically modified silica nanoparticles for gene delivery, *Int. J. Pharm.*, 2003, **266**, 51–60.
31 H. Sun, J. Zhao, B. Liu, J. Gou, H. He, Y. Zhang, T. Yin, X. Jin and X. Tang, Integrity of polymeric micelles regulates bioavailability of cyclosporine A: A FRET-based analysis during oral delivery, *J. Controlled Release*, 2025, **383**, 113831.
32 M. Abdulkarim, N. Agulló, B. Cattoz, P. Griffiths, A. Bernkop-Schnürch, S. G. Borros and M. Gumbleton, Nanoparticle diffusion within intestinal mucus: Three-dimensional response analysis dissecting the impact of particle surface charge, size and heterogeneity across polyelectrolyte, pegylated and viral particles, *Eur. J. Pharm. Biopharm.*, 2015, **97**, 230–238.
33 J. Rohrer, A. Partenhauser, S. Hauptstein, C. M. Gallati, B. Matuszczak, M. Abdulkarim, M. Gumbleton and A. Bernkop-Schnürch, Mucus permeating thiolated self-emulsifying drug delivery systems, *Eur. J. Pharm. Biopharm.*, 2016, **98**, 90–97.
34 A. Brotons-Canto, C. Gamazo, N. Martín-Arbella, M. Abdulkarim, J. Matías, M. Gumbleton and J. M. Irache, Evaluation of nanoparticles as oral vehicles for immunotherapy against experimental peanut allergy, *Int. J. Biol. Macromol.*, 2018, **110**, 328–335.
35 S. Bonengel, M. Jelkmann, M. Abdulkarim, M. Gumbleton, V. Reinstadler, H. Oberacher, F. Prüfert and A. Bernkop-Schnürch, Impact of different hydro-

phobic ion pairs of octreotide on its oral bioavailability in pigs, *J. Controlled Release*, 2018, **273**, 21–29.
36 J. Griesser, G. Hetényi, M. Moser, F. Demarne, V. Jannin and A. Bernkop-Schnürch, Hydrophobic ion pairing: Key to highly payloaded self-emulsifying peptide drug delivery systems, *Int. J. Pharm.*, 2017, **520**, 267–274.
37 C. Menzel, T. Holzeisen, F. Laffleur, S. Zaichik, M. Abdulkarim, M. Gumbleton and A. Bernkop-Schnürch, In vivo evaluation of an oral self-emulsifying drug delivery system (SEDDS) for exenatide, *J. Controlled Release*, 2018, **277**, 165–172.
38 X. Li, L. Li, X. Zhou, Y. Chen, Y. Ren, T. Zhou and W. Lu, Pharmacokinetic/pharmacodynamic studies on exenatide in diabetic rats, *Acta Pharmacol. Sin.*, 2012, **33**, 1379–1386.
39 X. Li, Z. Zhao, L. Li, T. Zhou and W. Lu, Pharmacokinetics, in vitro and in vivo correlation, and efficacy of exenatide microspheres in diabetic rats, *Drug Delivery*, 2015, **22**, 86–93.
40 L. Soudry-Kochavi, N. Naraykin, T. Nassar and S. Benita, Improved oral absorption of exenatide using an original nanoencapsulation and microencapsulation approach, *J. Controlled Release*, 2015, **217**, 202–210.
41 A. W. York, S. E. Kirkland and C. L. McCormick, Advances in the synthesis of amphiphilic block copolymers via RAFT polymerization: Stimuli-responsive drug and gene delivery, *Adv. Drug Delivery Rev.*, 2008, **60**, 1018–1036.
42 A. E. Smith, X. Xu and C. L. McCormick, Stimuli-responsive amphiphilic (co)polymers via RAFT polymerization, *Prog. Polym. Sci.*, 2010, **35**, 45–93.
43 W. Li, M. Nakayama, J. Akimoto and T. Okano, Effect of block compositions of amphiphilic block copolymers on the physicochemical properties of polymeric micelles, *Polymer*, 2011, **52**, 3783–3790.
44 G. Gaucher, M.-H. Dufresne, V. P. Sant, N. Kang, D. Maysinger and J.-C. Leroux, Block copolymer micelles: preparation, characterization and application in drug delivery, *J. Controlled Release*, 2005, **109**, 169–188.
45 Y. Cu and W. M. Saltzman, Controlled surface modification with poly(ethylene)glycol enhances diffusion of PLGA nanoparticles in human cervical mucus, *Mol. Pharm.*, 2010, **6**, 173–181.
46 M. Abdulkarim, P. K. Sharma and M. Gumbleton, Self-emulsifying drug delivery system: Mucus permeation and innovative quantification technologies, *Adv. Drug Delivery Rev.*, 2019, **142**, 62–74.
47 G. Moad, E. Rizzardo and S. H. Thang, Living Radical Polymerization by the RAFT Process—A First Update, *Aust. J. Chem.*, 2006, **59**, 669.
48 V. Strehmel, A. Laschewsky, H. Wetzel and E. Görnitz, Free Radical Polymerization of n-Butyl Methacrylate in Ionic Liquids, *Macromolecules*, 2006, **39**, 923–930.
49 K. Nakabayashi and H. Mori, Recent progress in controlled radical polymerization of N-vinyl monomers, *Eur. Polym. J.*, 2013, **49**, 2808–2838.
50 M. W. M. Fijten, R. M. Paulus and U. S. Schubert, Systematic parallel investigation of RAFT polymerizations for eight different (meth)acrylates: A basis for the designed synthesis of block and random copolymers, *J. Polym. Sci., Part A: Polym. Chem.*, 2005, **43**, 3831–3839.
51 X. Zhou, P. Ni, Z. Yu and F. Zhang, Latices of Poly(fluoroalkyl mathacrylate)-b-Poly(butyl methacrylate) Copolymers Prepared via Reversible Addition–Fragmentation Chain Transfer Polymerization, *J. Polym. Sci., Part A: Polym. Chem.*, 2007, **45**, 471–484.
52 R. Rojas, N. K. Harris, K. Piotrowska and J. Kohn, Evaluation of automated synthesis for chain and step-growth polymerizations: Can robots replace the chemists?, *J. Polym. Sci., Part A: Polym. Chem.*, 2009, **47**, 49–58.
53 S. M. Henry, A. J. Convertine, D. S. W. Benoit, A. S. Hoffman and P. S. Stayton, End-functionalized polymers and junction-functionalized diblock copolymers via RAFT chain extension with maleimido monomers, *Bioconjugate Chem.*, 2009, **20**, 1122–1128.
54 Z. Jia, C. Liu and J. Huang, Synthesis of (ABCB)n type ternary amphiphilic multiblock copolymer via poly(ethylene oxide) macro-chain transfer agent, *Polymer*, 2006, **47**, 7615–7620.
55 Y.-Z. You, C.-Y. Hong and C.-Y. Pan, A novel strategy for synthesis of multiblock copolymers, *Chem. Commun.*, 2002, 2800–2801.
56 V. Bütün, C. E. Bennett, M. Vamvakaki, A. B. Lowe, N. C. Billingham and S. P. Armes, Selective betainisation of tertiary amine methacrylate block copolymers, *J. Mater. Chem.*, 1997, **7**, 1693–1695.
57 C. Vauthier and K. Bouchemal, Methods for the Preparation and Manufacture of Polymeric Nanoparticles, *Pharm. Res.*, 2009, **26**, 1025–1058.
58 W. Lin, Z. Wang and S. Chen, in *Functional Polymers for Nanomedicine*, ed. Y. Shen, Royal Society of Chemistry, london, 2013, pp. 227–244.
59 J. P. Rao and K. E. Geckeler, Polymer nanoparticles: Preparation techniques and size-control parameters, *Prog. Polym. Sci.*, 2011, **36**, 887–913.
60 S. Galindo-rodriguez, E. Alle, H. Fessi and E. Doelker, Physicochemical Parameters Associated with Nanoparticle Formation in the Salting-out, Nanoprecipitation Methods, *Pharm. Res.*, 2004, **21**, 1428–1439.
61 A. J. Coupe, S. S. Davis and I. R. Wilding, Variation in gastrointestinal transit of pharmaceutical dosage forms in healthy subjects, *Pharm. Res.*, 1991, **8**, 360–364.
62 S. A. Galindo-Rodriguez, E. Allemann, H. Fessi and E. Doelker, Polymeric nanoparticles for oral delivery of drugs and vaccines: a critical evaluation of in vivo studies, *Crit. Rev. Ther. Drug Carrier Syst.*, 2005, **22**, 419–464.
63 S. Hornig, T. Heinze, C. R. Becer and U. S. Schubert, Synthetic polymeric nanoparticles by nanoprecipitation, *J. Mater. Chem.*, 2009, **19**, 3838.
64 K. Letchford and H. Burt, A review of the formation and classification of amphiphilic block copolymer nanoparticulate structures: micelles, nanospheres, nanocapsules and polymersomes, *Eur. J. Pharm. Biopharm.*, 2007, **65**, 259–269.

65 T. Riley, S. Stolnik, C. R. Heald, C. D. Xiong, M. C. Garnett, L. Illum, S. S. Davis, S. C. Purkiss, R. J. Barlow and P. R. Gellert, Physicochemical Evaluation of Nanoparticles Assembled from Poly(lactic acid)-Poly (ethylene glycol) (PLA-PEG) Block Copolymers as Drug Delivery Vehicles, *Langmuir*, 2001, **17**, 3168–3174.

66 C. Heald, S. Stolnik and K. Kujawinski, Poly (lactic acid)-poly (ethylene oxide)(PLA-PEG) nanoparticles: NMR studies of the central solidlike PLA core and the liquid PEG corona, *Langmuir*, 2002, 3669–3675.

67 A. B. Lowe, N. C. Billingham and S. P. Armes, Synthesis and Properties of Low-Polydispersity Poly (sulfopropylbetaine)s and Their Block Copolymers, *Macromolecules*, 1999, **32**, 2141–2148.

68 Z. Tuzar, H. Pospisil, J. Plestil, A. B. Lowe, F. L. Baines, N. C. Billingham and S. P. Armes, Micelles of hydrophilic-hydrophobic poly(sulfobetaine)-based block copolymers, *Macromolecules*, 1997, **30**, 2509–2512.

69 E. Muro, T. Pons, N. Lequeux, A. Fragola, N. Sanson, Z. Lenkei and B. Dubertret, Small and stable sulfobetaine zwitterionic quantum dots for functional live-cell imaging, *J. Am. Chem. Soc.*, 2010, **132**, 4556–4557.

70 J. P. Priebe, M. L. Satnami, D. W. Tondo, B. S. Souza, J. M. Priebe, G. a. Micke, A. C. O. Costa, H. D. Fiedler, C. a. Bunton and F. Nome, The chameleon-like nature of zwitterionic micelles: The intrinsic relationship of anion and cation binding in sulfobetaine micelles, *J. Phys. Chem. B*, 2008, **112**, 14373–14378.

71 J. a Pedro, J. R. Mora, M. Silva, H. D. Fiedler, C. a Bunton and F. Nome, Surface charge of zwitterionic sulfobetaine micelles with 2-naphthol as a fluorescent probe, *Langmuir*, 2012, **28**, 17623–17631.

72 T. S. J. Kashi, S. Eskandarion, M. Esfandyari-Manesh, S. M. A. Marashi, N. Samadi, S. M. Fatemi, F. Atyabi, S. Eshraghi and R. Dinarvand, Improved drug loading and antibacterial activity of minocycline-loaded PLGA nanoparticles prepared by solid/oil/water ion pairing method, *Int. J. Nanomed.*, 2012, **7**, 221–234.

73 B. Gupta, B. K. Poudel, S. Pathak, J. W. Tak, H. H. Lee, J.-H. Jeong, H.-G. Choi, C. S. Yong and J. O. Kim, Effects of Formulation Variables on the Particle Size and Drug Encapsulation of Imatinib-Loaded Solid Lipid Nanoparticles, *AAPS PharmSciTech*, 2015, 1–11.

74 K. S. Chu, A. N. Schorzman, M. C. Finniss, C. J. Bowerman, L. Peng, J. C. Luft, A. J. Madden, A. Z. Wang, W. C. Zamboni and J. M. DeSimone, Nanoparticle drug loading as a design parameter to improve docetaxel pharmacokinetics and efficacy, *Biomaterials*, 2013, **34**, 8424–8429.

75 W. Abdelwahed, G. Degobert, S. Stainmesse and H. Fessi, Freeze-drying of nanoparticles: Formulation, process and storage considerations, *Adv. Drug Delivery Rev.*, 2006, **58**, 1688–1713.

76 F. De Jaeghere, E. Allémann, J. C. Leroux, W. Stevels, J. Feijen, E. Doelker and R. Gurny, Formulation and lyoprotection of poly(lactic acid-co-ethylene oxide) nanoparticles: influence on physical stability and in vitro cell uptake, *Pharm. Res.*, 1999, **16**, 859–866.

77 A. Laschewsky, Structures and synthesis of zwitterionic polymers, *Polymers*, 2014, **6**, 1544–1601.

78 N. I. Lebovka, in *Polyelectrolyte Complexes in the Dispersed and Solid State I Principles and Theory*, ed. M. Müller, Springer Berlin Heidelberg, Berlin, 2012, pp. 57–96.

79 G. I. Guerrero-García, P. González-Mozuelos and M. Olvera De La Cruz, Large counterions boost the solubility and renormalized charge of suspended nanoparticles, *ACS Nano*, 2013, **7**, 9714–9723.

80 T. G. F. Souza, V. S. T. Ciminelli and N. D. S. Mohallem, A comparison of TEM and DLS methods to characterize size distribution of ceramic nanoparticles, *J. Phys.: Conf. Ser.*, 2016, **733**, 012039.

81 S. Pabisch, B. Feichtenschlager, G. Kickelbick and H. Peterlik, Effect of interparticle interactions on size determination of zirconia and silica based systems – A comparison of SAXS, DLS, BET, XRD and TEM, *Chem. Phys. Lett.*, 2012, **521**, 91–97.

82 C. M. Maguire, M. Rösslein, P. Wick and A. Prina-Mello, Characterisation of particles in solution – a perspective on light scattering and comparative technologies, *Sci. Technol. Adv. Mater.*, 2018, **19**, 732–745.

83 S. M. Garg, M. R. Vakili and A. Lavasanifar, Polymeric micelles based on poly(ethylene oxide) and α-carbon substituted poly(ε-caprolactone): An in vitro study on the effect of core forming block on polymeric micellar stability, biocompatibility, and immunogenicity, *Colloids Surf., B*, 2015, **132**, 161–170.

84 A. Veeren, A. Bhaw-Luximon and D. Jhurry, Polyvinylpyrrolidone–polycaprolactone block copolymer micelles as nanocarriers of anti-TB drugs, *Eur. Polym. J.*, 2013, **49**, 3034–3045.

85 Y. Bae, N. Nishiyama, S. Fukushima, H. Koyama, M. Yasuhiro and K. Kataoka, Preparation and Biological Characterization of Polymeric Micelle Drug Carriers with Intracellular pH-Triggered Drug Release Property: Tumor Permeability, Controlled Subcellular Drug Distribution, and Enhanced in Vivo Antitumor Efficacy, *Bioconjugate Chem.*, 2005, **16**, 122–130.

86 X. Li, Y. Zhang, Y. Fan, Y. Zhou, X. Wang, C. Fan, Y. Liu and Q. Zhang, Preparation and evaluation of novel mixed micelles as nanocarriers for intravenous delivery of propofol, *Nanoscale Res. Lett.*, 2011, **6**, 275.

87 A. Choucair, C. Lavigueur and A. Eisenberg, Polystyrene-b-poly(acrylic acid) Vesicle Size Control Using Solution Properties and Hydrophilic Block Length, *Langmuir*, 2004, **20**, 3894–3900.

88 N. Bailly, G. Pound-Lana and B. Klumperman, Synthesis, Characterization, and Self-Assembly of Poly(N-vinylpyrrolidone)-block-poly(vinyl acetate), *Aust. J. Chem.*, 2012, **65**, 1124.

89 S. Yu, T. Azzam, I. Rouiller and A. Eisenberg, "Breathing" Vesicles, *J. Am. Chem. Soc.*, 2009, **131**, 10557–10566.

90 D. E. Discher and A. Eisenberg, Polymer Vesicles, *Science*, 2002, **297**, 967–973.

91 Y. Chang, W. Chang, Y. Shih, T. Wei and G. Hsiue, Zwitterionic Sulfobetaine-Grafted Poly (vinylidene fluoride) Membrane with Highly Effective Blood Compatibility via Atmospheric Plasma-Induced Surface Copolymerization, *ACS Appl. Mater. Interfaces*, 2011, **3**, 1228–1237.
92 H. Sun, M. Y. Z. Chang, W. I. Cheng, Q. Wang, A. Commisso, M. Capeling, Y. Wu and C. Cheng, Biodegradable zwitterionic sulfobetaine polymer and its conjugate with paclitaxel for sustained drug delivery, *Acta Biomater.*, 2017, **64**, 290–300.
93 L. He, S. Li, C. T. W. Chung, C. Gao and J. H. Xin, Constructing safe and durable antibacterial textile surfaces using a robust graft-to strategy via covalent bond formation, *Sci. Rep.*, 2016, **6**, 36327.
94 Z. Zhang, T. Chao, L. Liu, G. Cheng, B. D. Ratner and S. Jiang, Zwitterionic hydrogels: An in vivo implantation study, *J. Biomater. Sci., Polym. Ed.*, 2009, **20**, 1845–1859.
95 A. Muheem, F. Shakeel, M. A. Jahangir, M. Anwar, N. Mallick, G. K. Jain, M. H. Warsi and F. J. Ahmad, *Saudi Pharm. J.*, 2016, **24**, 413–428.
96 A. Patel, M. Patel, X. Yang and A. Mitra, Recent Advances in Protein and Peptide Drug Delivery: A Special Emphasis on Polymeric Nanoparticles, *Protein Pept. Lett.*, 2014, **21**, 1102–1120.
97 F. Tong, Preparation of exenatide-loaded linear poly(ethylene glycol)-brush poly(l-lysine) block copolymer: Potential implications on diabetic nephropathy, *Int. J. Nanomed.*, 2017, **12**, 4663–4678.
98 S. Dünnhaupt, O. Kammona, C. Waldner, C. Kiparissides and A. Bernkop-Schnürch, Nano-carrier systems: Strategies to overcome the mucus gel barrier, *Eur. J. Pharm. Biopharm.*, 2015, **96**, 447–453.
99 J. Della Rocca and W. Lin, *Nanomedicine*, 2012, **7**, 303–305.
100 S. S. D'Souza and P. P. DeLuca, Methods to assess in Vitro drug release from injectable polymeric particulate systems, *Pharm. Res.*, 2006, **23**, 460–474.
101 S. Modi and B. D. Anderson, Determination of drug release kinetics from nanoparticles: Overcoming pitfalls of the dynamic dialysis method, *Mol. Pharm.*, 2013, **10**, 3076–3089.
102 S. S. D'Souza and P. P. DeLuca, Development of a dialysis in vitro release method for biodegradable microspheres, *AAPS PharmSciTech*, 2005, **6**, E323–E328.
103 A. Sood and R. Panchagnula, Peroral route: An opportunity for protein and peptide drug delivery, *Chem. Rev.*, 2001, **101**, 3275–3303.
104 M. L. Tan, P. F. M. Choong and C. R. Dass, Recent developments in liposomes, microparticles and nanoparticles for protein and peptide drug delivery, *Peptides*, 2010, **31**, 184–193.
105 F. Hintzen, G. Perera, S. Hauptstein, C. Müller, F. Laffleur and A. Bernkop-Schnürch, In vivo evaluation of an oral self-microemulsifying drug delivery system (SMEDDS) for leuprorelin, *Int. J. Pharm.*, 2014, **472**, 20–26.
106 B. Zhang, D. He, Y. Fan, N. Liu and Y. Chen, Oral delivery of exenatide via microspheres prepared by cross-linking of alginate and hyaluronate, *PLoS One*, 2014, **9**, 1–7.
107 L. Soudry-Kochavi, N. Naraykin, T. Nassar and S. Benita, Improved oral absorption of exenatide using an original nanoencapsulation and microencapsulation approach, *J. Controlled Release*, 2015, **217**, 202–210.
108 D. Parkes, Pharmacokinetic actions of exendin-4 in the rat: Comparison with glucagon-like peptide-1, *Drug Dev. Res.*, 2001, **53**, 260–267.
109 H. N. Nguyen, S. P. Wey, J. H. Juang, K. Sonaje, Y. C. Ho, E. Y. Chuang, C. W. Hsu, T. C. Yen, K. J. Lin and H. W. Sung, The glucose-lowering potential of exendin-4 orally delivered via a pH-sensitive nanoparticle vehicle and effects on subsequent insulin secretion in vivo, *Biomaterials*, 2011, **32**, 2673–2682.
110 P. Enck, V. Merlin, J. F. Erckenbrecht and M. Wienbeck, Stress effects on gastrointestinal transit in the rat, *Gut*, 1989, **30**, 455–459.
111 R. Guignet, G. Bergonzelli, V. Schlageter, M. Turini and P. Kucera, Magnet Tracking: A new tool for in vivo studies of the rat gastrointestinal motility, *Neurogastroenterol. Motil.*, 2006, **18**, 472–478.
112 M. Anitha, G. Sakthidevi, S. Muthukumarasamy and V. R. Mohan, Effect of cynoglossum zeylanicum (vehl ex Hornem) thunb. ex lehm on oral glucose tolerance in rats, *J. Appl. Pharm. Sci.*, 2012, **2**, 75–78.
113 K. Tatarkiewicz, C. Polizzi, C. Villescaz, L. J. D'Souza, Y. Wang, S. Janssen and D. G. Parkes, Combined antidiabetic benefits of exenatide and dapagliflozin in diabetic mice, *Diabetes, Obes. Metab.*, 2014, **16**, 376–380.